

Review

Recent Development of Pd-Based Electrocatalysts for Proton Exchange Membrane Fuel Cells

Hui Meng ^{1,*}, Dongrong Zeng ¹ and Fangyan Xie ²

¹ Department of Physics and Siyuan Laboratory, College of Science and Engineering, Jinan University, Guangzhou 510632, China; E-Mail: zengdongrong_jnu@163.com

² Instrumental Analysis & Research Center, Sun Yat-sen University, Guangzhou 510275, China; E-Mail: xiefy@mail.sysu.edu.cn

* Author to whom correspondence should be addressed; E-Mail: tmh@jnu.edu.cn; Tel.: +86-20-8522-4386; Fax: +86-20-8522-0233.

Academic Editor: Minhua Shao

Received: 7 May 2015 / Accepted: 6 July 2015 / Published: 15 July 2015

Abstract: This review selectively summarizes the latest developments in the Pd-based catalysts for low temperature proton exchange membrane fuel cells, especially in the application of formic acid oxidation, alcohol oxidation and oxygen reduction reaction. The advantages and shortcomings of the Pd-based catalysts for electrocatalysis are analyzed. The influence of the structure and morphology of the Pd materials on the performance of the Pd-based catalysts were described. Finally, the perspectives of future trends on Pd-based catalysts for different applications were considered.

Keywords: fuel cells; catalyst; palladium

1. Introduction

Fuel cells convert chemical energy directly into electrical current without combustion. The first article illustrating such a device was published at the end of the 1830s [1], and the interest in this field has been growing since the 1950s [2]. Among various types of the low-temperature fuel cells, proton exchange membrane fuel cells (PEMFCs) are attractive power sources for portable, automotive and stationary applications due to their high energy density, high efficiency and low operating temperature. Comparing with H₂ as fuel, the liquid fuels such as formic acid and ethanol have special advantage in

storage and transport, which can find better applications in portable devices and make use of current gasoline system. The direct formic acid fuel cells (DFAFCs) have an open circuit potential of 1.190 V and energy density of 2086 Wh L⁻¹. The formic acid is non-toxic and has small crossover flux. The shortcoming of DFAFCs is their relatively low energy density. Compared with formic acid, ethanol has much higher energy density of 8030 Wh kg⁻¹. However, ethanol suffers from the sluggish reaction kinetics.

The electrochemical oxidation of fuels requires the use of a catalyst to achieve the high current densities for practical applications. Platinum (Pt) is the mostly used catalyst in the PEMFCs. However, the vast commercialization of fuel cell is hindered by the high cost and low reserve of Pt. The kinetics of the oxygen reduction reaction (ORR), which is the cathode reaction of a fuel cell is slow on Pt. Moreover, Pt is easy to be poisoned without recovery by the intermediates of the reaction of the impurities from the fuel or oxidant. Particularly in some types of PEMFCs, Pt is not the best choice. For example, in direct formic acid fuel cells (DFAFCs), the oxidation of formic acid is quite low due to the poisoning of the Pt by the CO-like intermediates during the reaction. In direct ethanol fuel cells (DEFCs), the poor utilization and the poisoning of Pt catalyst particularly in alkaline solution also limits its applications. The electrocatalytic activities of the ethanol oxidation reaction could be significantly improved in alkaline media on Pd-based catalyst which have comparable or even better electrocatalytic activity than that of Pt-based catalyst. The ORR is one of the key reactions in fuel cells with the higher overpotential compared with the anode reactions. Pt group metal based catalysts are currently used for PEMFCs to reduce the large ORR overpotential. Unfortunately, even on the active Pt surface, the overpotential is over 200 mV at open circuit voltage (OCV). Pd is another active metal for the ORR. Binary Pd-base metal systems have been identified as promising PEMFC cathode catalyst with the enhanced activity for ORR and stability compared with Pd alone [3].

Pd has an electronic configuration identical to Pt and forms a not very strong bond to most adsorbates. The key differences are that the *d* bands of Pd are closer to the cores than that of Pt. There are less *d* electron densities available for bonding. This leads to weaker interactions with *d* bonds, which allows unique chemistry to occur. Pd has higher oxidation potential than Pt and the Pd oxides are more stable. Weak inter-atomic bonds between Pd atoms compared with Pt lead to easier formation of the subsurface species. Also, Pd has a very similar lattice constant to that of Pt. The electrocatalysis of formic acid on a Pd single crystal surface could be significantly enhanced as the *d*-band centre of Pd shifted down with an appropriate value due to the modest lattice compressive strain. All these electronic properties make Pd a promising alternative to Pt or even better than Pt in many situations.

From the recent 5-year price change of the Pd, its price has changed from one fourth to two fifths of the Pt [4]. However, Pd still has some advantages considering the reservation and price. As one of the most studied materials, Pd has attracted considerable interest for its applications in many fields. Similar to Pt, most of the Pd is used in the automotive industry for catalytic converters to reduce the toxicity of emissions from a combustion engine. Pd also has vast applications in electronic, dental and jewelry. Only a small percentage of Pd is used in chemistry. In electrochemistry, Pd nanoparticles are very important catalyst, especially for the oxidation of formic acid, ethanol oxidation in alkaline solution, hydrogen oxidation and the ORR. Pd-based catalyst for alcohol oxidation have been reviewed in 2009 [5]. Another review paper in 2009 reviewed the application of Pd in fuel cell anode and cathode [6]. However, the Pd-based fuel cells are still very hot in recent years. We have surveyed

the 270 published papers on the Pd-based catalysts in recent four years from 2009 to 2014 and the distribution of the papers was as shown in Figure 1. Seven review papers were published after 2009. Two review papers published in 2010 partly concerned the application of Pd in fuel cells [7,8]. Morozan *et al.*, reviewed the application of Pd in fuel cells [9]. Recently Shao reviewed Pd as catalyst for hydrogen oxidation and oxygen reduction reaction [3]. Zhao *et al.*, reviewed the catalysts for direct methanol fuel cells including the application of Pd [10]. Adams and Chen's review paper focused on the application of Pd in hydrogen storage [11]. The nano-structure of Pd for catalysis and hydrogen storage was also reviewed recently by Zhou in *Chem. Soc. Rev.* [12]. Analyzing recent review papers on Pd-based catalysts, it was found that there was no comprehensive review paper concerning the application of Pd in fuel cells. This review analyzed the latest four years' publications on Pd catalyst for proton exchange membrane fuel cells and provides a comprehensive review on the recent development of the Pd-based catalysts for formic acid oxidation, alcohol oxidation and oxygen reduction reaction.

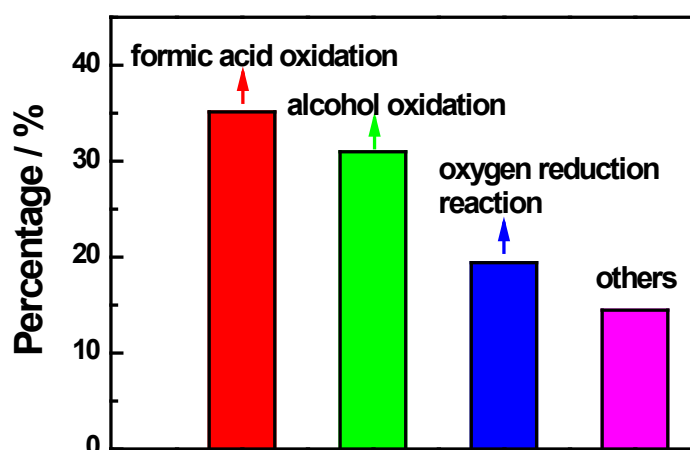


Figure 1. The distribution of Pd in recent four years in fuel cell technologies.

Based on our survey, in all the published papers on Pd-based catalysts, 35.12% is for the the formic acid oxidation, 30.99% for alcohol oxidation and 19.42% for ORR as shown in Figure 1. Therefore, this review article mainly focuses on the recent development of the Pd-based catalysts, particularly, on these three most important reactions. This survey result also shows the possible areas where Pd can compete with or replace Pt in PEMFCs. Besides above aspects, the control of the morphology and crystallography of Pd and the corresponding effect on catalysis are also reviewed.

2. Pd Nanostructures

The development of nanotechnology makes it possible to control the morphology and crystallography of Pd nanostructures, which has been proven to affect the catalytic activity. Crystalline surfaces with a high density of low-coordinated atoms are generally superior in catalytic activity and stability to flat planes that are composed of closely packed surface atoms. This makes nanoparticle possible to show high activity and stability at very small Pd loadings if the nanoparticles are controllably synthesized as an open-structured surfaces with high density of low-coordinated atoms. The availability of

the open-structured surfaces comes from the morphology of the material, so the shape control of the nanocrystals has become one of the crucial challenges.

2.1. The 0-D Pd Structures

Zero-dimensional (0-D) Pd structures include nano-particles, quantum dots, atomic cluster and nanoclusters and so on. The nano-particles are the most often used structure for fuel cell applications, Pd can be prepared into nano-particles which are usually called “Pd black” or Pd nano-particles loaded on support materials. Both Pd black and the supported Pd nano-particles are widely used as fuel cell catalysts. Other than the common ball-like particles, the particles with multifacets attracted much attention since their unique crystallographic and morphologic structures, which greatly improved the activity and stability when used as fuel cell catalysts. With a square-wave potential method Tian *et al.* [13] electrodeposited tetrahedral Pd nanocrystals with $\{730\}$ high-index facets. With similar technique, Zhou *et al.* [14] prepared the Pd NCs not limited to the tetrahedral crystals. Shen *et al.* [15] used a sonoelectrochemical method to prepare Pd spherical nanoparticles, multitwinned particles, and spherical spongelike particles. Ding *et al.* [16] prepared single crystalline Pd nanocubes with the polyol method. Porous Pd nanoflowers were prepared by a liquid phase approach [17]. The above Pd particles all show improved mass activity or specific activity in fuel cell reactions, for example the tetrahedral Pd shows 4-6 times enhancement of specific activity and 1.5–3 times enhancement of mass activity in ethanol oxidation compared with commercial Pd particles on carbon [13].

The morphology of the crystal is determined by the internal features of a crystal, but the relationship between the crystalline structure and crystalline shape is still an unresolved problem. It still needs a correlation between crystallographic structure, morphological evolution and resultant shape of the nanocrystals. Zhou *et al.* [14] proposed the correlation between crystalline planes and nanocrystalline shape. There is a triangle relationship between the unit stereographic of fcc single-crystal and the surface atomic arrangement. There is also an intrinsic triangle that coordinates the crystalline surface index and the shape of the metal, which is shown in Figure 2.

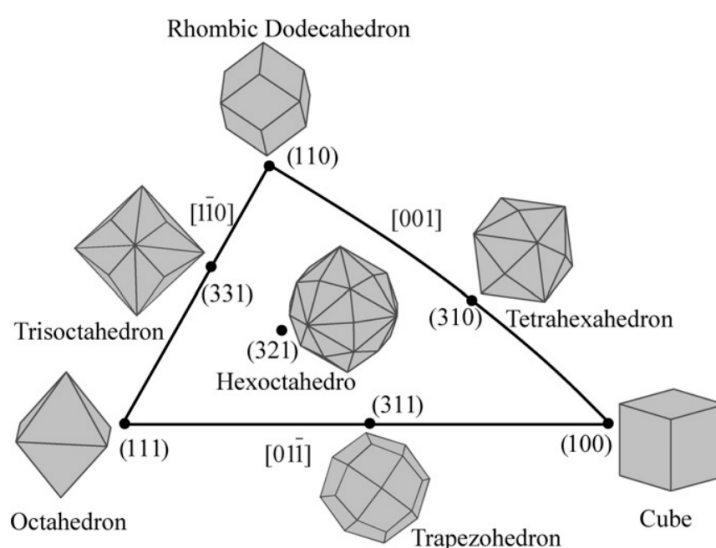


Figure 2. Unit stereographic triangle of polyhedral nanocrystals bounded by different crystal planes. Reproduced with permission from reference [14].

2.2. The 1-D Pd Structures

Compared with nanoparticess, one-dimensional (1-D) materials such as the nanowires, nanothorns and nanotubes offer unique benefits including (1) anisotropic morphology; (2) thin metal catalyst layer which leads to higher mass transport of the reactants; (3) high aspect ratio which is immune to surface energy driven coalescence via crystal migration; (4) less vulnerable to dissolution, Ostwald ripening and aggregation during the electrocatalytic process due to their micrometer-sized length; (5) high electrochemical active areas. Therefore, the 1-D structures are also intensively studied. Meng *et al.* [18,19] synthesized Pd single-crystal nanothorns along the $\langle 220 \rangle$ direction with a square wave electrochemical reduction method as shown in Figure 3. The nanothorn was made by a succession of epitaxial dodecahedrons of decreasing sizes aligned in the direction of the (111) plane and the growth of the thorn occurs along the (220) plane. Tian *et al.* [20] obtained five fold twinned Pd nanorods with high-index facets of $\{hkk\}$ or $\{hk0\}$. Patra *et al.* [21] prepared Pd dendrite branches growing along the $\langle 110 \rangle$ directions. According to the mechanism proposed by different authors, the Pd thorns obtained from different methods might share similar mechanism in the crystal growth [21]. It has been proposed that the breaking of symmetry leads to the formation of one-dimensional nanostructure, which facilitates the formation of one specific facet as the bounding side facet in the nanostructure. The formation of a tapered structure implies that the specific facet has a high surface step density to accommodate the change in diameter.

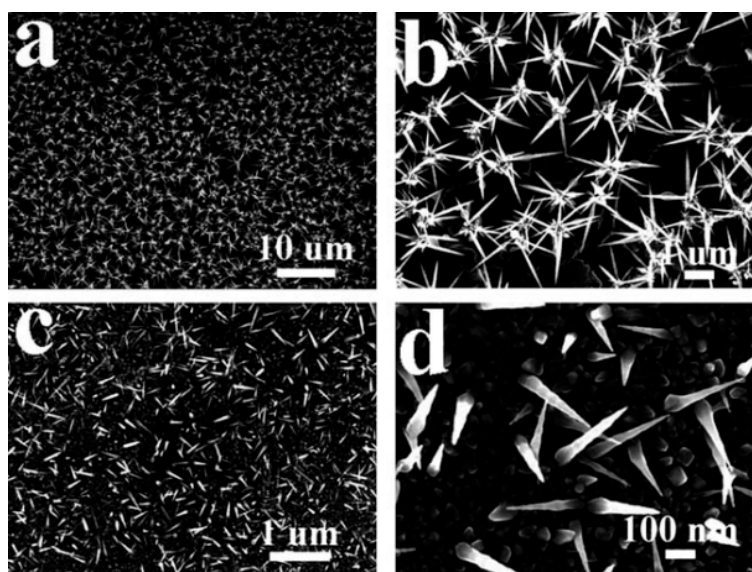


Figure 3. SEM micrographs of pure Pd thorn clusters (a,b) and the mixture of Pd thorns and Pd particles (c,d). Reproduced with permission from reference [19].

Besides the preparation of nanothorns without templates or surfactants, other 1-D structures such as the nanorods, nanotube and nanowires can be prepared based on the templates such as anodic aluminum oxide (AAO) [22]. Du *et al.* [23] prepared porous Pd-based alloy nanowires with AAO. Lee *et al.* [24] prepared Pd nanotubes with ZnO nanowires as sacrificial templates. The nanotube structures have large surface areas and it is expected to show enhanced catalytic efficiencies. Wen *et al.* [25] used Te NWs as sacrificial template to prepare ultrathin Pd nanowires. The Pd nanowire or nanotube forms nanoporous

metallic structure with high surface area, unique chemical properties and interconnected structures that do not require any support to avoid the corrosion and detachment problems common for carbon supported catalysts.

2.3. The 3-D Pd Structures

Compared with two-dimensional (2-D) structure, the three-dimensional (3-D) structure often has high porosity which will lead to higher surface area, especially higher electrochemical active surface area. Usually, the 2-D structure is very few used in the fuel cell application. Jena *et al.* [26] explored the synthesis of 3-D porous Pd nanostructures with a various shapes and morphologies. These structures have high surface roughness and surface steps which can contribute to the increased accessibility of reactant species and are more attractive for enhancing catalytic application. Zhou *et al.* [27] and Yu *et al.* [28] produced dendritic structures by electrochemical deposition. The authors concluded that the morphology of the electrochemically deposited nanostructured Pd could be solely controlled by tuning the depositing potentials. Fang *et al.* [29] reported an electrochemical route to synthesize Pd nanourchins. Li *et al.* [30] synthesized Pd/Au hollow cone-like microstructures by electrodeposition. Ye *et al.* [31,32] fabricated a three-dimensional mesoporous Pd networks by a simple reduction method in solution using a face centered cubic silica super crystal as template. From above analysis, it is concluded that the electrochemical synthesis is a useful tool in the preparation of Pd nanostructures without templates or surfactants. Many structures such as the high index facets enclosed nanoparticles, nanothorns and dendritic structures were prepared by the electrodeposition.

2.4. Hollow or Core-Shell Structures

The hollow nanomaterials have big potentials for further reducing the cost. Moreover, they have distinguished chemical and physical properties resulting from their special shape and composition [33,34]. Liu *et al.* [35] and Bai *et al.* [36] prepared raspberry hollow Pd nanospheres by a galvanic replacement reaction involving Co nanoparticles as sacrificial template. The raspberry surface might be helpful in increasing the surface area for catalysis. The core-shell structure is effective to reduce cost by reducing the amount of Pd used in the catalyst. Fang *et al.* [37] prepared the Au@Pd@Pt structure with a gold core, a Pd shell and Pt clusters on the shell as shown in Figure 4. The optimized structure had only two atomic layers of Pd and a half-monolayer equivalent of Pt. The activity was critically dependent upon the Pd-shell thickness and the Pt-cluster coverage. The high activity originated from the synergistic effect existing between the three different nanostructure components (sphere, shell and islands). Ksar *et al.* [38–40] synthesized bimetallic Pd-Au nanostructures with a core rich in gold and a Pd porous shell. This structure greatly reduced the loading of Pd. The addition of Au to Pd catalysts was not only improved the catalytic activity and selectivity but also enhanced the resistance to poisoning.

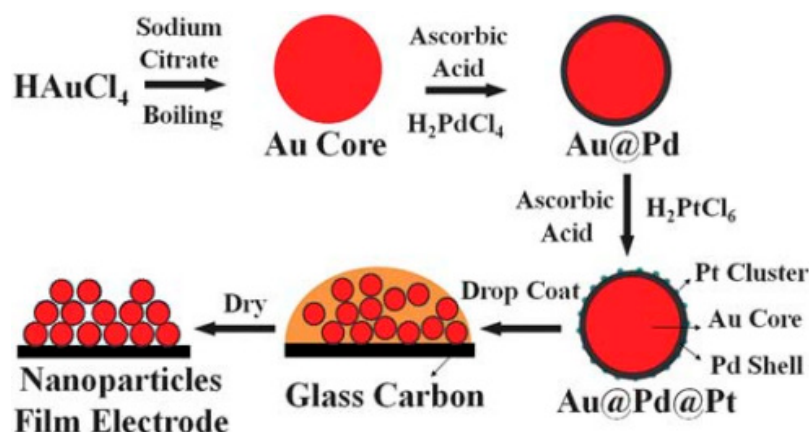


Figure 4. The procedure used to prepare an Au@Pd@Pt NP film on a glass carbon (GC) electrode. Reproduced with permission from reference [37].

2.5. Conclusions and Perspective Discussions

With the development of nanotechnology, researchers are able to control the morphology of Pd in nanoscale. Different morphologies such as particles with multi-facets, cubes, twinned particles, assembled particles, nanorods, nanothorns, nanowires, nanotubes, dendritic structure, networks and hollow/core-shell structures and so on have been successfully prepared. Most of the Pd nanomaterials have high performance in fuel cell half cell characterization, which is caused by the unique crystallography and morphology of the material. Both the activity and stability of the electrochemical reaction could be improved when catalyzed by the Pd nanomaterials to significantly reduce the usage of Pt in fuel cells. However, the research on Pd nanostructures is still in the fundamental stage and great efforts need to be done to apply these nanomaterials into the real fuel cell applications. With the development of nano-synthesis technology there will be more morphologies with unique advantages prepared, emphasis should be put on the controlled synthesis and application in fuel cell membrane electrode assembly application.

3. Pd-Based Catalysts for the Direct Formic Acid Fuel Cells (DFAFCs)

The direct formic acid fuel cells (DFAFCs) have a high theoretical open circuit potential of 1.450 V compared with 1.229 V for H_2 proton exchange membrane fuel cells (PEMFCs) and 1.190 V for direct methanol fuel cells (DMFCs) at room temperature. The formic acid is a non-toxic liquid fuel and lower crossover flux than methanol and ethanol. Although the net energy density of formic acid (2086 Wh L^{-1}) is lower than that of methanol (4690 Wh L^{-1}), high concentrated formic acid can be used as fuel, e.g., 20 M (70 wt. %), compared with lower methanol concentration, e.g., 1–2 M. Therefore, formic acid carries more energy per volume than methanol. The formic acid itself is an electrolyte and can facilitate proton transport within anode compartment [41].

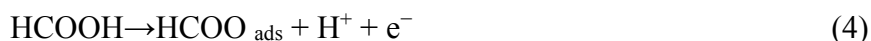
It was reported that Pd/C exhibited much better activity compared with Pt/C, however, the activity was not satisfactory and more importantly the durability of Pd/C catalyst was in urgent need for further improvement. Generally, formic acid oxidation on Pd or Pt surface follows a dual pathway mechanism, namely, a dehydration pathway [42–44]:



and a dehydrogenation one:



On Pt catalyst, formic acid oxidation also took place via the third pathway with bridge bonded adsorbed formate intermediate being in equilibrium with the solution formats [36–38].



Pd has a propensity to break only the O–H bonds of the HCOOH molecule in the entire potential region, while, Pt has a propensity to break the C–O and/or C–H bond (at low overpotential) and the O–H bond (at high overpotential). Consequently, formic acid oxidation on Pd surfaces proceeds exclusively through the dehydrogenation reaction step, whereas, on Pt surfaces the dehydration pathway is predominant at low potentials. It should be noted that one of the major problems in formic acid oxidation is that the intermediary species formed during the oxidation of HCOOH cause catalyst poisoning. These intermediate species could be mostly CO, which strongly interacts with the active sites on the electrode surface and requires a higher overpotential for oxidation to CO₂. On a Pt catalyst, formic acid decomposition proceeds mainly via a dehydration pathway where the strongly adsorbed CO greatly hinders the catalytic activity. On pure Pt surfaces, CO poisoning due to the dehydration of formic acid on at least two or more contiguous Pt atoms hinders the direct dehydrogenation oxidation of formic acid at lower overpotentials. In contrast, formic acid decomposition on a Pd catalyst mainly proceeds in a dehydrogenation pathway. The generation of minor CO on the surfaces of Pd nanoparticles leads to the rapid decay of the catalytic activity. Hence, it is of great importance to design a Pd catalyst with excellent CO tolerance. For HCOOH oxidation, Pd shows superior initial performance compared with Pt. However, the high performance cannot be sustained, as Pd dissolves in acidic solutions and is vulnerable towards intermediate species. Modification of Pd with foreign metal has been considered as an effective method to enhance the activity and durability towards HCOOH oxidation. Studies have shown that the Pd oxidation activity for formic acid is also strongly influenced by the morphology and size of the Pd nanoparticles.

Table 1 listed the available data of the formic acid oxidation on Pd-based catalyst described in the literature. Three factors were compared: the electrochemical active surface area (EASA), the peak potential of formic acid oxidation and the peak current density of formic acid oxidation. According to the results provided by different authors, the EASA varied from the minimum of 15.7 m² g⁻¹ to the maximum of 208.2 m² g⁻¹. The peak current density varied from 3900 to 56.5 mA mg⁻¹_{Pd}, or from 159 to 12.4 mA cm⁻². The peak potential analysis showed that the alloying of the Pd with other metals could reduce the overpotential for formic acid oxidation as evidenced by the negative shift of the peak potential on the alloys. Alloying with other metals can modify the electronic structure and induce tensile strain of the Pd clusters, and finally influence their catalytic activities. The highest peak current density observed on Pd_{0.9}Pt_{0.1}/C is nearly twice as high as that on Pd/C and six times as that on the commercial Pt/C [45]. The anodic peak current density obtained by using PdCo/MWCNTs as catalyst is 3 and

4.3 times higher than Pd/MWCNTs and Pd/XC-72 [46]. PdNi₂ alloy had almost three times the activity of Pd, even if the molar Pd content in PdNi₂ alloy was only one third of pure Pd [47].

Table 1. Details of the half cell performance of the Pd-based catalysts.

Catalysts	EASA/m ² g ⁻¹	Peak Potential/V	Peak Current	Conditions H ₂ SO ₄ /Formic Acid/Scan Rate	References
		RHE	Density/mA mg ⁻¹ Pd		
Pt@Pd/C	156.5	0.277	3900	0.5 M/2 M/10 mV s ⁻¹	[48]
Pt/C	198	0.687	/	0.5 M/2 M/10 mV s ⁻¹	[48]
Pd/C	208.2	0.417	1200	0.5 M/2 M/10 mV s ⁻¹	[48]
butylphenyl-stabilized Pd	122	0.38	3390	0.1 M/0.1 M/100 mV s ⁻¹	[49]
Pd black	33.6	0.46	750	0.1 M/0.1 M/100 mV s ⁻¹	[49]
butylphenyl-stabilized Pd	122	0.38	3390	0.1 M/0.1 M/100 mV s ⁻¹	[49]
PdPt/C	49	/	2500	0.5 M/0.5 M/50 mV s ⁻¹	[50]
Pd/C	/	/	2400	0.1 M/0.5 M/20 mV s ⁻¹	[51]
Pd/C	107.2	/	1426.5	0.5 M/0.5 M/50 mV s ⁻¹	[52]
PdSn/C	/	/	1420	0.5 M/0.5 M/20 mV s ⁻¹	[53]
Pd/C	/	/	610	0.5 M/0.5 M/20 mV s ⁻¹	[53]
Pd/CMRT	67.27	/	1140 at 0.44 V *	0.5 M/0.5 M/50 mV s ⁻¹	[54]
Pd/RT	41.47	/	670 at 0.44 V *	0.5 M/0.5 M/50 mV s ⁻¹	[54]
Pd/C	63.72	/	440 at 0.44 V *	0.5 M/0.5 M/50 mV s ⁻¹	[54]
Pd/HPMo-PDDA-MWCNT	/	/	945	0.5 M/0.5 M/20 mV s ⁻¹	[55]
Pd/AO-MWCNTs	/	/	554	0.5 M/0.5 M/20 mV s ⁻¹	[55]
Pd/C	/	/	373	0.5 M/0.5 M/20 mV s ⁻¹	[55]
Pd ₅₇ Ni ₄₃	/	/	830	0.5 M/0.5 M/50 mV s ⁻¹	[23]
Pd/C	/	/	700	0.5 M/0.5 M/50 mV s ⁻¹	[23]
Pd-PANI	/	/	822	0.5 M/0.2 M/100 mV s ⁻¹	[56]
PdAu	90	/	800	0.5 M/0.5 M/20 mV s ⁻¹	[57]
Pd/C	43	/	250	0.5 M/0.5 M/20 mV s ⁻¹	[57]
Pd/graphene	72.72	/	446.3	0.5 M/0.5 M/50 mV s ⁻¹	[58]
Pd/C	31.85	/	191.9	0.5 M/0.5 M/50 mV s ⁻¹	[58]
Pd/graphene	/	0.39	300	0.5 M/0.5 M/50 mV s ⁻¹	[59]
Pd/C	/	/	193	0.5 M/0.5 M/50 mV s ⁻¹	[59]
Pd networks	/	/	275.4	0.5 M/0.5 M/50 mV s ⁻¹	[31]
Nanoporous Pd	23	/	262	0.5 M/0.5 M/10 mV s ⁻¹	[60]
Pd/CNT	/	0.44	200 at 0.27 V *	0.5 M/0.5 M/50 mV s ⁻¹	[61]
Pt/CNT	/	0.92	30 at 0.27 V *	0.5 M/0.5 M/50 mV s ⁻¹	[61]
Pt Pd/CNT	/	0.64	50 at 0.27 V *	0.5 M/0.5 M/50 mV s ⁻¹	[61]
Pt ₁ Pd ₃ /CNT	/	0.64	125 at 0.27 V *	0.5 M/0.5 M/50 mV s ⁻¹	[61]
PdSn/C	64.7	/	170.2	0.5 M/1 M/10 mV s ⁻¹	[62]
Pd/C	39.8	/	102.3	0.5 M/1 M/10 mV s ⁻¹	[62]
Pd black	/	/	56.5	0.5 M/0.5 M/50 mV s ⁻¹	[31]
Pd/untreated-MWCNT	46.2	0.517	159 mA cm ⁻²	0.5 M/0.5 M/50 mV s ⁻¹ with glutamate	[63]
Pd/acid-oxidized MWCNT	35.7	/	108 mA cm ⁻²	0.5 M/0.5 M/50 mV s ⁻¹	[63]
Pd/untreated-MWCNT	21.4	/	72 mA cm ⁻²	0.5 M/0.5 M/50 mV s ⁻¹ without glutamate	[63]
PdNi/C	/	0.247	105.1 mA cm ⁻²	0.5 M/1 M/10 mV s ⁻¹	[64]

Table 1. Cont.

Catalysts	EASA/m ² g ⁻¹	Peak Potential/V	Peak Current	Conditions H ₂ SO ₄ /Formic Acid/Scan Rate	References
		RHE	Density/mA mg ⁻¹ Pd		
Pd/C	/	0.287	72.9 mA cm ⁻²	0.5 M/1 M/10 mV s ⁻¹	[64]
PdCo/MWCNTs	/	0.28	107 mA cm ⁻²	0.5 M/0.1 M/20 mV s ⁻¹	[46]
Pd/MWCNTs	/	0.32	35.6 mA cm ⁻²	0.5 M/0.1 M/20 mV s ⁻¹	[46]
Pd/XC-72	/	0.38	24.8 mA cm ⁻²	0.5 M/0.1 M/20 mV s ⁻¹	[46]
Pd _{0.9} Pt _{0.1} /C	83	0.35	87.5 mA cm ⁻²	0.5 M/0.5 M/50 mV s ⁻¹	[45]
Pt/C	85.6	0.52	15.1 mA cm ⁻²	0.5 M/0.5 M/50 mV s ⁻¹	[45]
Pd/C	89.7	0.48	42.5 mA cm ⁻²	0.5 M/0.5 M/50 mV s ⁻¹	[45]
Pd-B/C	87.6	/	65.4 mA cm ⁻²	0.5 M/0.5 M/50 mV s ⁻¹	[65]
Pd/C	90	/	36.0 mA cm ⁻²	0.5 M/0.5 M/50 mV s ⁻¹	[65]
Pd-Au/C	/	0.37	18.6 mA cm ⁻²	0.5 M/0.5 M	[66]
Pd/C	/	0.48	12.4 mA cm ⁻²	0.5 M/0.5 M	[66]
Pd/phen-MWCNTs	37.6	/	/	0.5 M/1 M/50 mV s ⁻¹	[67]
Pd/AO-MWCNTs	15.7	/	/	0.5 M/1 M/50 mV s ⁻¹	[67]
Pd/graphene	44	0.367	/	1 M/1 M/10 mV s ⁻¹	[68]
Pd/Vulcan C	35	0.377	/	1 M/1 M/10 mV s ⁻¹	[68]

* The potentials were vs. RHE.

3.1. Pd Supported on Carbon Materials

3.1.1. Pd on Carbon Powders

An active catalyst should be dispersed on a convenient support to stabilize the catalytic nanoparticles, to obtain optimum catalyst utilization and to reduce the amount of precious metal used, reducing the catalyst cost. In DFAFCs, highly conductive carbon materials such as Vulcan XC-72 carbon (Cabot, Boston, MA, USA) provide a high dispersion of metal nanoparticles to facilitate electron transfer, resulting in better catalytic activity. The supported electrocatalyst is a practical means to achieve high utilization of expensive noble metals and to maintain good life-time. Other carbon materials such as the carbon fiber are also studied as support material for palladium [69–71].

There are still aspects to improve in the Pd/C as catalyst in fuel cell applications. The works usually focus on the Pd particle size control via novel synthesis techniques to achieve high electrochemical active surface area and improve the utilization efficiency of the Pd catalyst. Cheng *et al.* [72] prepared highly dispersed Pd/C catalyst through an ambient aqueous way instead of the traditional high temperature polyol process in ethylene glycol. The Pd/C catalyst without stabilizer had a higher oxidation activity toward formic acid compared with that of a traditionally prepared Pd/C catalyst. Liang *et al.* [52] synthesized a highly dispersed and ultrafine carbon-supported Pd nanoparticle catalyst which exhibited significantly high electrochemical active surface area and high electrocatalytic performance for formic acid oxidation with four times larger formic acid oxidation current compared with that prepared by general NaBH₄ reduction method. The large electrochemical specific surface may be due to the high dispersion and small particle size of Pd/C catalyst. Suo *et al.* [73] used a simple and stabilizer-free ethylene glycol reduction method to prepare Pd/C catalyst. Size-dependent electrochemical property was observed and electrochemical evaluation showed that Pd/C with a particle

size of 6.1 nm performed the highest activity for formic acid oxidation. The performance of the Pd/C catalyst for the oxidation of formic acid could be greatly promoted with 3.19 times enhancement in catalytic stability and 1.57 times improvement in the catalytic activity by simply introducing vanadium ions in very low concentration to the electrolyte [51]. The improvement in the catalytic performance may be attributed to the facilitating of formic acid oxidation due to the existence of $\text{VO}^{2+}/\text{V}^{3+}$ redox pair and the ensemble effect induced by the adsorption of vanadium ions onto the surface of Pd.

3.1.2. Pd alloys on Carbon Powders

Pd displays an initial high activity for the oxidation of HCOOH. However, its long term performance is poor. Deactivation of Pd activity has been assigned to catalyst poisoning by CO, although, other poisoning species such as anions from the electrolyte can also be effective. Alloying Pd with the second metal to change the surface electronic state, an ensemble effect could occur, which could possibly reduce the catalyst poisoning and increase the activity and lifetime of the catalyst.

(1) PdPt alloys

It was found $\text{Pd}_{0.9}\text{Pt}_{0.1}/\text{C}$ was the optimum catalyst for the desired formic acid oxidation reaction [45]. The highest peak current density observed on $\text{Pd}_{0.9}\text{Pt}_{0.1}/\text{C}$ was nearly twice as high as that on Pd/C and six times as that on the commercial Pt/C, which is superior to any reported carbon black-supported Pt/C, Pd/C, and $\text{Pt}_x\text{Pd}_{1-x}/\text{C}$ catalysts. There is also a large negative shift (up to 0.21 V) in peak potential for a $\text{Pd}_x\text{Pt}_{1-x}/\text{C}$ versus that for Pd/C. The high performance of the $\text{Pd}_{0.9}\text{Pt}_{0.1}$ nanoalloy can be ascribed to the effectively inhibited CO poisoning at largely separated Pt sites and appropriately lowered *d*-band centre of Pd sites. The addition of Pt to Pd considerably improved the steady-state activity of Pd [74–76]. Chronoamperometric measurements showed that the most active catalyst was $\text{Pd}_{0.5}\text{Pt}_{0.5}$ with the particle size of 4 nm. Wu *et al.* [48] prepared a Pd decorated Pt/C catalyst, Pt@Pd/C, with a small amount of Pt as core. It was found that the catalyst showed excellent activity toward anodic oxidation of formic acid at room temperature and its activity was 60% higher than that of Pd/C. It is speculated that the high performance of Pt@Pd/C may result from the unique core-shell structure and synergistic effect of Pt and Pd at the interface. Wang *et al.* [50] decorated Pd/C with Pt nanoparticles where the amount of three neighbouring Pt or Pd atoms markedly decreased. As a result, discontinuous Pd and Pt atoms suppressed CO formation and exhibited unprecedented catalytic activity and stability toward formic acid oxidation.

(2) PdSn alloys

Liu *et al.* [77] prepared Pd and PdSn nanoparticles supported on Vulcan XC-72 carbon by a microwave-assisted polyol process. It was found that the addition of Sn to Pd could increase the lattice parameter of the Pd (fcc) crystal. The PdSn/C catalysts have higher electrocatalytic activity for formic acid oxidation than a comparative Pd/C catalyst. The $\text{Pd}_2\text{Sn}_1/\text{C}$ catalyst exhibited higher current density and enhanced electrocatalytic stability compared with Pd/C. There was also a negative shift of the peak potential on $\text{Pd}_2\text{Sn}_1/\text{C}$ than that of Pd/C. Zhang *et al.* [53] synthesised PdSn/C catalysts with different atomic ratios of Pd to Sn. The alloy catalysts exhibited significantly higher catalytic activity and stability for formic acid oxidation than that of Pd/C catalyst. Pd was modified by Sn through an electronic effect which could decrease the adsorption strength of the poisonous intermediates on Pd and thus promote

the formic acid oxidation. Tu *et al.* [62] prepared a carbon-supported PdSn (PdSn/C) catalyst with greatly improved performance for formic acid oxidation compared with that of Pd/C. Adding Sn at a small ratio into the carbon-supported Pd catalyst could largely increase the current density of the formic acid oxidation and shift the onset potential toward the negative compared with that of Pd/C. The reason for the improvement of the catalyst was likely attributed to the high dispersion of the Pd and due to the change in the electronic properties of the Pd.

(3) Other alloys

Zhang *et al.* [66] prepared carbon-supported PdAu catalysts with different alloying degree. The electrocatalytic activity of PdAu/C catalyst for the formic acid oxidation was strongly dependent on the alloying degree of Pd-Au nanoparticles. The PdAu/C catalyst with higher alloying degree showed a higher electrocatalytic activity and stability for the formic acid oxidation compared with the PdAu/C catalyst at lower alloying degree, which can be ascribed to the enhancement of CO tolerance and possible suppression of the dehydration pathway in the course of formic acid oxidation. The catalytic activity of the PdAu/C catalyst was also found to be affected by the nature of the supporting materials [78–81]. Gao *et al.* [64,82,83] synthesized carbon-supported PdNi catalyst by sodium borohydride reduction reaction. The performance of the PdNi/C catalyst for formic acid oxidation was significantly improved compared with that of Pd/C. The potential of the main anodic peak of formic acid at PdNi/C catalyst electrode was about 40 mV more negative than that at Pd/C catalyst electrode. The onset potential of formic acid oxidation at PdNi/C catalyst electrode was 30 mV more negative than that at Pd/C catalyst electrode. The reason for the promotion effect may be due to that Ni can contribute to the adsorption of oxygen-containing species, which is conducive to the oxidation of formic acid and a change in electronic properties of Pd. Yu *et al.* [84] prepared carbon supported bimetallic PdPb catalysts which were found to be more resistant to deactivation in the DFAFC than Pd/C and to consistently show better long-term performance. The addition of Pb to Pd stabilized it significantly to deactivation during formic acid oxidation. Wang *et al.* [65] synthesized highly dispersed boron-doped Pd nanoparticles supported on carbon black with high Pd loadings (*ca.* 40 wt. % Pd) by using NaBH₄ as the reductant. The as-prepared Pd-B/C catalyst showed extraordinary high activity toward formic acid oxidation compared with that of a commercially available Pd/C catalyst. Thermal treatment further enhanced the durability of the oxidation current on Pd-B/C. The superior performance of the Pd-B/C catalyst may arise from uniformly dispersed nanoparticles within optimal size ranges, the increase in surface-active sites, and the electronic modification effect of boron species. The Pd–Co, PdCeO_x/C [85] and PtRu/C [86–88] catalyst also exhibited excellent catalytic activity and stability in the oxidation of formic acid.

3.1.3. Pd Supported on Carbon Nanotubes

It remains a challenge to load Pd nanoparticles on the surface of carbon nanotubes because of the graphitization of carbon nanotubes. However, due to the advantages of carbon nanotubes especially in the contribution to stability of the catalyst, many works are devoted to the deposition of Pd on carbon nanotubes [89,90]. Hu *et al.* [63] synthesized Pd nanoparticles supported on untreated multiwalled carbon nanotubes (MWCNTs). The Pd/MWCNT catalyst displayed superior electrocatalytic activity

and stability in formic acid oxidation. Chakraborty *et al.* [91] synthesized nanosized Pd particles supported on MWCNTs. Bai *et al.* [67,92] functionalized MWCNTs with 1,10-phenanthroline (phen-MWCNTs) as a catalyst support for Pd nanoparticles. It was found that Pd nanoparticles were evenly deposited without obvious agglomeration, and the average particle size of the Pd nanoparticles was only as small as 2.3 nm. The as-prepared Pd/phen-MWCNTs catalyst had a better electrocatalytic activity and stability for the oxidation of formic acid than Pd catalyst on acid treated MWCNTs. Phen made a strong impact on the electrocatalytic activity of the catalyst through the functionalization of the MWCNTs and the formation of the active Pd-N sites. Therefore, the dispersivity and the ESA of the Pd nanoparticles were obviously enhanced in the presence of phen, resulting in better electrocatalytic activity and utilization efficiency of the catalyst. Cui *et al.* [55] loaded Pd nanoparticles on phosphomolybdic (HPMo) acid functionalized multiwalled carbon nanotubes supports. The catalysts exhibited a much higher electrocatalytic activity and stability for formic acid oxidation reaction as compared with that on traditional Pd/C. The high electrocatalytic activities were most likely related to highly dispersed and fine Pd nanoparticles as well as synergistic effect between Pd and HPMo immobilized on functionalized MWCNTs.

3.1.4. Pd Alloys Supported on Carbon Nanotubes

(1) PdPt alloys

Selvaraj *et al.* [93,94] prepared PtPd nanoparticles supported on purified singlewalled carbon nanotubes. The modified electrode exhibited significantly high electrocatalytic activity toward formic acid oxidation due to the uniform dispersion of nanoparticles on SWCNTs and the efficacy of Pd species in Pt-Pd system. Winjobi *et al.* [61] prepared Pt, Pd and Pt_xPd_y alloy nanoparticles supported on carbon nanotubes with high and uniform dispersion. With increasing Pd amount of the catalysts, the mass activity of formic acid oxidation reaction on the CNT supported catalysts increased. A direct oxidation pathway of formic acid oxidation occurred on the Pd surface, while, the formic acid oxidation was through CO_{ads} intermediate pathway on the Pt surface. The Pd/CNT demonstrated 7 times better mass activity than that of Pt/CNT at an applied potential of 0.27 V (vs. RHE) in the chronoamperometry test.

(2) PdAu alloys

Chen *et al.* [95] prepared PdAu/multiwalled carbon nanotubes (Pd-Au/MWCNTs) to increase the stability and performance of the Pd-based catalysts in DFAFCs. The catalyst was highly active in formic acid oxidation, due to the hydrogen treated catalysts have smaller metal particles and better contact with MWCNTs support. When Pd was alloyed with Au the leaching of Pd was considerably slower, which may be caused by much slower Pd leaching from Pd-Au alloy than from Pd. The Pd-Au/MWCNTs had higher current and lower onset potential for formic acid oxidation than Pd/MWCNTs. Chen *et al.* [96] prepared multiwalled carbon nanotubes (MWCNTs) supported Pd-Au catalyst for oxidation of formic acid and compared with a similarly prepared Pd/MWCNTs and a commercial Pt-Ru/C catalyst. Both the Pd-Au/MWCNTs and the Pd/MWCNTs catalysts used were more active than that of a commercial Pt-Ru/C catalyst. The specific activity of Pd in the novel Au-Pd/MWCNTs catalyst was over two times higher than that on the Pd/MWCNTs catalyst. Mikolajczuk *et al.* [97] found that the Pd-Au/MWCNTs catalyst exhibited higher activity and more

stable in oxidation reaction of formic acid. The higher initial catalytic activity of Pd-Au/MWCNTs catalyst than Pd/MWCNTs catalyst in formic acid oxidation reaction was attributed to the electronic effect of gold in Pd-Au alloy [98,99].

(3) Other alloys

Morales-Acosta *et al.* [46,100] compared the Pd-Co and Pd catalysts prepared by the impregnation synthesis method on MWCNTs. The current density achieved with the PdCo/MWCNTs catalyst was 3 times higher than that of the Pd/MWCNTs catalyst. The onset potential for formic acid oxidation on PdCo/MWCNTs catalyst showed a negative shift *ca.* 50 mV compared with Pd/MWCNTs. The anodic peak current density obtained by using PdCo/MWCNTs was 3 and 4.3 times higher than Pd/MWCNTs and Pd/C, respectively. The PdCo/MWCNTs exhibited good stability in acidic media, higher current density and more negative anodic potential associated to this reaction than that of Pd/MWCNTs and Pd/C catalysts. The difference could be attributed to a better dispersion of the metallic nanoparticles with a lower particle size achieved with the MWCNTs-supported materials. Specific surface area obtained from PdCo and Pd supported on MWCNTs was higher than that obtained on Pd supported on Vulcan XC-72 carbon.

3.1.5. Pd Supported on Graphene

Graphene is a rapidly rising star on the horizon of the materials science and technology which has attracted tremendous attention and holds great promise for advanced fields. Especially in fuel cells, the emergence of graphene has opened a new avenue for utilizing two-dimensional planer carbon material as a catalytic support owing to its high conductivity, unique graphitized basal plane structure. This is propitious to not only maximize the availability of nanosized electrocatalyst surface area for electron transfer but also provide better mass transport of reactants to the electro-catalyst [101]. Fu *et al.* [59] developed an effective surfactant-free strategy for the small-sized Pd particles deposited on graphen. The Pd/GN catalyst exhibited excellent catalytic activity and stability toward formic acid oxidation compared with the Pd/C catalysts [102]. The enhanced performance of the Pd/GN catalyst was contributed to the small size and high dispersion of Pd NPs and the stabilizing effect of the graphene support. While the group has also fabricated the Pd/graphene hybrid via sacrifice template route [58]. Bong *et al.* [68] synthesized high loadings of 80 wt% Pd on graphene catalysts which showed significantly enhanced electrocatalytic activity and stability for formic acid oxidation compared with Pd/C catalysts.

3.2. Pd Supported on Oxides

As alternatives to improve the catalytic activity and stability of the Pd-based catalysts, the carbon support materials were modified with semiconducting oxides, such as TiO₂, MoO_x and SnO₂ [103–105]. The influence of TiO₂ support on the electronic effect and the bifunctional mechanism can be summarized as follows. (1) TiO₂ support imposes an electronic effect in which the hypo-*d*-electronic titanium ions promote the electrocatalytic properties of hyper-*d*-electronic noble metal surface atoms, thus lowering the adsorption energy of CO intermediates and increasing the mobility of the CO group on Pd nanostructures; (2) Adsorption of OH species (OH_{ad}) on TiO₂ can facilitate the conversion of

the catalytically poisonous CO intermediates into CO₂, thereby improving the durability of Pd catalysts. Additionally, TiO₂ can facilitate the dispersion of noble metal nanoparticles to anchor them. Based on the theory that TiO₂ nanoparticles in the catalyst can adsorb OH_{ads} species and promote the oxidation reaction on the electrode, Xu *et al.* [44] prepared highly dispersed carbon supported Pd-TiO₂ catalyst with intermittent microwave irradiation. The activity of Pd-TiO₂/C catalyst for the oxidation of formic acid was higher than that of the Pd/C catalyst [106]. Wang *et al.* [54] investigated Pd nanoparticles supported on carbon-modified rutile TiO₂ (CMRT) as catalyst for formic acid oxidation. The Pd/CMRT showed three times the catalytic activity of Pd/C, as well as better catalytic stability toward formic acid oxidation. The enhanced catalytic property of Pd/CMRT mainly arises from the improved electronic conductivity of the carbon-modified rutile TiO₂, the dilated lattice constant of Pd nanoparticles, an increasing of surface steps and kinks in the microstructure of Pd nanoparticles and slightly better tolerance to the adsorption of poisonous intermediates [107]. Wang *et al.* [108] investigated the influence of the crystal structure of TiO₂ supporting material on formic acid oxidation. TiO₂ with the rutile structure improved the catalytic activity of Pd nanoparticles toward formic acid oxidation. The enhancement of Pd/TiO₂ (rutile) catalytic activity arose from uniform dispersion of Pd nanoparticles, an increase in surface-active sites, and good tolerance to the adsorption of poisonous intermediates (such as CO_{ad}, COOH_{ad} and so on). This study proved that rutile TiO₂ was a better supporting material than anatase TiO₂ or composites.

3.3. Pd Supported on other Supporting Materials

At present, carbon nanotubes (CNTs) and Vulcan XC-72 carbon are the most often used supporting materials to load Pd nanoparticles. However, the rate of formic acid oxidation is lower partly due to lower Pd utilization on such conventional carbon supports, which is related to the lower electrochemically accessible surface area for the deposition of Pd particles. Tremendous efforts have been devoted to search for new catalyst supports to achieve good dispersion, utilization, activity and stability [109]. Bai *et al.* [110] supported Pd nanoparticles on polypyrrole-modified fullerene and the Pd/ppy-C₆₀ catalyst showed a good electrocatalytic activity and stability for the oxidation of formic acid. Pd on polyaniline (Pd-PANI) nanofiber film [56], on polypyrrole (PPy) film [111] and PMo₁₂ [112] showed excellent catalytic activity in the oxidation reaction of formic acid in acidic media. Qin *et al.* [113] synthesized highly dispersed and active Pd/carbon nanofiber (Pd/CNF) catalyst which exhibited good catalytic activity and stability for the oxidation of formic acid. Cheng *et al.* [114] loaded Pd nanoparticles on the carbon nanoparticle-chitosan host, the chitosan matrix was shown to be beneficial in making nanosized catalyst convenient, effective, and reproducible. The Pd on carbon nanoparticle-chitosan host catalysts was highly active for the oxidation of formic acid.

3.4. Unsupported Pd

Based on the practical application of Pd based catalysts in fuel cells, Pd is usually supported on other materials. However, since the nanotechnology provides the possibility to control the morphology of Pd material, and the intrinsic properties of the nanostructured material can be dramatically enhanced by shape and structural variations, there are also some research on the preparation of unsupported Pd materials for fuel cell application [115–117]. The one-dimensional Pd nanostructures like nanowires,

nanobelts and nanotubes have attracted significant interest due to their exotic technological applications. Wang *et al.* [60] and Ye *et al.* [31] fabricated unsupported nanoporous Pd networks which exhibited high electrochemical active specific surface area, and high catalytic activity for oxidation of formic acid. Pd hollow nanostructures is an efficient way to reduce the cost of catalyst, for example Pd/Au hollow cone-like microstructures [30] and Pd clusters on highly dispersed Au nanoparticles [57] are found to show superior performance at much lower cost. Alloyed nanowires such as PdNi₂ [47] and Pd₅₇Ni₄₃ [23] alloy nanowires also shows improved performance. The size and nature of surface structures, such as crystalline planes and surface ligands is one key issue to improve the mass activity. Zhou *et al.* [49] synthesized monodispersed butylphenyl-functionalized Pd (Pd-BP) nanoparticles with unique surface functionalization and a high specific electrochemical surface area (122 m² g⁻¹), the Pd-BP nanoparticles exhibited a mass activity of 4.5 times as that of commercial Pd black for HCOOH oxidation as shown in Figure 5. The Pd-BP catalyst shows obvious improvement in both activity and stability compared with commercial Pd-black.

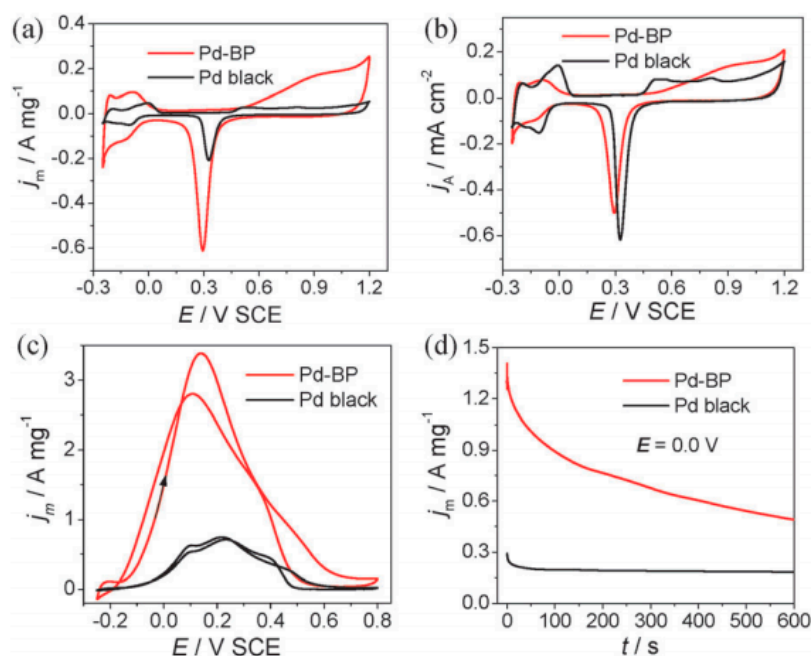


Figure 5. Cyclic voltammograms of butylphenyl-functionalized Pd (Pd-BP) nanoparticles and commercial Pd black in 0.1 M H₂SO₄, with the currents normalized (a) by the mass loadings of Pd and (b) by the effective electrochemical surface areas at a potential scan rate of 100 mV s⁻¹; Panels (c) and (d) depict the cyclic voltammograms and current-time curves acquired at 0.0 V for HCOOH oxidation, respectively, at the Pd-BP nanoparticles and Pd black-modified electrode in 0.1 M HCOOH + 0.1 M H₂SO₄ at room temperature. Reproduced with permission from reference [49].

3.5. Single Fuel Cell Characterization

3.5.1. Single Fuel Cell Performance

The aim of the study on the Pd based catalyst is to realize its practical application in fuel cells. However, because of the difference in the preparation technique of the membrane electrode assembly

(MEA) it is relatively difficult to compare the performance of a catalyst. The single fuel cell performance of the different catalysts was selectively summarized in Figure 6. Meng *et al.* [118] designed a novel MEA structure for DFAFCs where Pd nanothorns were directly electrodeposited onto the carbon paper to form the anode catalyst layer. The novel MEA provided 2.4 times higher peak power density than that of the conventional MEA. The increase in the performance was due to the improved mass transport of the formic acid in the catalyst and diffusion layers, better Pd utilization and higher electroactivity of the Pd single crystal nanothorns. Cheng *et al.* [119] electrodeposited Pd on graphite felt (GF) and the resulting catalyst was compared with Pt-Ru/GF for the oxidation of formic acid. The Pd/GF anode reached 852 W m^{-2} compared to 392 W m^{-2} with a commercial Pd catalyst-coated membrane (CCM). Mikołajczuk *et al.* [42] prepared a new carbon black supported Pd catalyst for DFAFC applications. The maximum power density of the novel 10 wt. % Pd catalyst was only 23% lower than that of the commercial 20 wt. % Pd/C. Pd-Au on multiwalled carbon nanotubes (MWCNTs) exhibited higher power density and better stability in DFAFC than that of the similar Pd/MWCNTs catalyst [79]. The 17.8 wt. % Pd/MWCNTs catalyst reached three times of the peak power density compared with that of a 20 wt. % Pt-Ru/C catalyst [120]. A MEA of the Pd/MWCNTs catalyst showed a power density of 3.3 mW cm^{-2} with 50% less Pd loadings than that of commercial Pd/C [121]. The addition of Pb and Sb into the Pd black catalyst caused a strong promotion for the formic acid oxidation in a cell [43]. Yu *et al.* [122] systematically evaluated and compared a number of carbon-supported Pt-based and Pd-based catalysts with commercial Pd/C, PtRu/C, and Pt/C catalysts in a multi-anode DFAFC. It is found that the PdBi/C provided higher stability than that of the commercial Pd/C catalyst, while both of the PdMo/C and PdV/C catalysts provided poor cell performances. The results provided strong evidence that both Mo and V poison Pd through electronic and/or chemical effects. Based on above analysis and Figure 6 it can be concluded that alloying with another metal is an efficient way to improve the performance of Pd based catalyst in direct formic acid fuel cell full cell performance, as is evidenced by the PdSn or Pd Sb alloy [98,123]. Next to the alloy is the Pd black with lower performance than the alloy. Pd nanothorns prepared by a novel electrodeposition technique shows higher performance than most Pd black, showing the effect of morphology control on catalytic activity. However the unexpected conclusion is Pd or Pd alloy supported on novel carbon supports such as graphene and carbon nanotube does not show much improvement in the performance. The conclusion points out further aspects to be explored in this field: try to realize the morphology or crystallography control of Pd nanostructure aiming at high activity and stability, try to load the novel nanostructure on carbon support material aiming at reduce the loading amount of Pd, finally reducing the cost.

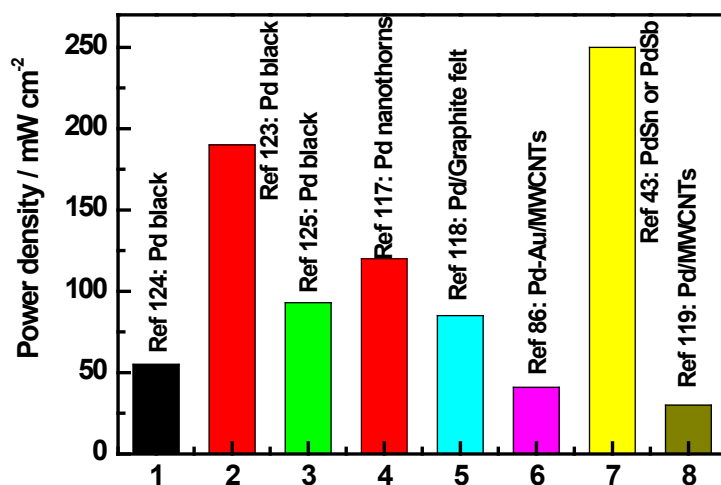


Figure 6. Comparison of the power density of the single fuel cell performance with selected catalysts.

3.5.2. Deactivation Mechanism and Reactivation

The limited durability of Pd-based anode for DFAFCs has seriously restricted their practical application. The mechanistic clarification on how to remove the poisoning species and to reactivate the Pd-based anode still remains a big challenge. The major factors causing performance degradation in the DFAFCs are an increment in the anode charge-transfer resistance and a growth in the particle size of the Pd anode catalyst [124]. The anode charge-transfer resistance, confirmed by EIS, increases with the operation time due to poisoning of the catalyst surface. The performance loss caused by surface poisoning could be completely recovered by the reactivation process. However, the increase in the catalyst size induces a reduction in active surface area and the performance loss caused by the growth in catalyst size cannot be recovered by the reactivation process. The deactivation of Pd/C increases sharply with increasing the formic acid concentration but only depends on the potential at high cell voltages. Reactivation can be achieved by driving the cell voltage to a reverse polarity of -0.2 V or higher. Although the reason for the activity loss is still unclear, it has been found that almost full activity can be recovered by applying an anodic potential of *ca.* 1.0 V *vs.* RHE or more. Ren *et al.* [125] found that the Pd oxides/hydrous oxides (POHOs) play a crucial role in promoting better performance and minimizing performance degradation of the Pd-based DFAFCs. The intrinsic presence or introduction of Pd oxides/hydrous oxides during catalysis of formic acid oxidation was found to promote elimination of poisoning species, thereby leading to a better performance of DFAFCs. Zhou *et al.* [126] found that Pd catalyst poisoned at the anode of a DFAFC under constant current discharging could be fully regenerated by a non-electrochemical method, *i.e.*, just switching pure water to DFAFC for 1 h. The voltage variation during the regeneration showed that one platform of 0.35 V was formed by the intermediate species of formic acid oxidation, which is proven to be critical for cell performance regeneration. The results indicated that the absorption of poisoning species on Pd was the main reason for the decaying of cell performance. Yu *et al.* [127] systematically studied the deactivation and electrochemical reactivation of a carbon supported Pd catalyst. The reactivation can be accomplished within a matter of seconds at ≥ 1.0 V *vs.* DHE (cell voltage ≤ -0.3 V). However, reactivation at a cell voltage of 0 V or higher is required from a practical perspective. Analyzing above results it is concluded that the decaying of

the cell performance is mainly caused by two factors: one is the growth of Pd particle size and the other is the absorption of poisoning species on Pd surface. The performance loss caused by surface poisoning could be recovered by the reactivation process, while the loss caused by particle growth can not be recovered. So how to limit the growth of particle size becomes one crucial problem in the stability study of the Pd based catalyst.

4. Pd-Based Catalysts for the Direct Ethanol Fuel Cells (DEFCs)

Among the alcohols, methanol and ethanol are the two most commonly used fuels for direct alcohol fuel cells (DAFCs). Direct ethanol fuel cell (DEFC) has attracted significant attention since ethanol is non-toxic, naturally available, renewable, and higher power density comparing to methanol (8030 Wh kg⁻¹ for ethanol and 6100 Wh kg⁻¹ for methanol). However, the sluggish reaction kinetics of ethanol oxidation is still a challenge to the commercialization of DEFC. There are many difficulties associated with ethanol oxidation and consequently in its use in fuel cell. Complete oxidation of ethanol to CO₂ involves 12 electrons and the process involves the scission of a C–C bond thus demanding high activation energies to be overcome. Many of the intermediates (mainly CO and –CHO) produced during the oxidation reaction poison the anode catalyst and in turn reduce the catalytic efficiency. Pt-based catalysts are recognized as the best catalysts for low temperature fuel cells. However, the high cost and limited resource of Pt limited its use as catalysts. At the same time, the poor utilization and the poisoning of Pt catalyst particularly in alkaline solution also limited its applications. A great deal of interest has recently been focused on the cheaper materials than platinum and the use of non-noble transition metals in alkaline media, in particular, the performance of alloys of Pd with non-noble metals for the oxidation of ethanol. In acidic environment, the complete oxidation of ethanol is difficult and the catalytic activities of the catalysts for ethanol oxidation reaction (EOR) could be significantly improved in alkaline media, where Pd-based catalyst has comparable or even better catalytic activity compared with Pt-based catalysts for ethanol oxidation [128,129]. This is why that the Pd-based materials are intensively studied for the oxidation of ethanol.

Table 2 summarized the key factors of the EOR including the specific activity, the mass activity, the onset potential and the peak potential. It was found that the mass activity of Pd for ethanol oxidation could reach as high as 2200 A g⁻¹_{Pd} [130]. Such high activity originated from the higher utilization of Pd and at the same time the reduced metal content. The mass activity could be even higher for the alloys if the current was only account by the mass of Pd. Alloying with other metals, especially, Ni could improve the kinetics of the ethanol oxidation as revealed by the negatively shifted onset potential and peak potential [131–133]. The construction of the core-shell structure was found to be an effective way to reduce the overpotential [38]. It is found that the Ru@PtPd/C [134] and Pd–Ni–Zn/C [135] show highest mass activity in the EOR, implying the advantages of multi-alloy and core-shell structure. Two components alloying of Pd with other metals have been intensively studied, while the multi-alloying still needs to be put more attention, and the multi-alloying also provides vast variations in the choice and combination of different metals. Novel nanostructure of Pd is still a popular topic in this field [136–141].

Table 2. Details of the ethanol oxidation on Pd catalysts. (SA: Specific Activity; MA: Mass Activity; OP: Onset Potential and PP: Peak Potential).

Catalysts	SA ¹ /mA cm ⁻²	MA ² /A g ⁻¹ _{Pd}	OP ³ /V RHE	PP ⁴ /V RHE	Conditions Ethanol/KOH/Scan Rate	References
Dendritic Pd	17	/	-0.353	-0.003	1 M/1 M/20 mV s ⁻¹	[28]
Pd/CNTs	/	800	-0.353	0.007	0.5 M/0.5 M/50 mV s ⁻¹	[35]
Pd shell/Au core	0.890	/	-0.582	-0.15	1 M/1 M/50 mV s ⁻¹	[38]
Pd/HCHs	42	2200	-0.352	-0.072	2 M/1 M/50 mV s ⁻¹	[130]
PdNPs/CFCNT	16	/	-0.24	0.14	1 M/1 M/60 mV s ⁻¹	[136]
Pd-In ₂ O ₃ /CNTs	61	/	-0.347	-0.022	1 M/0.5 M/50 mV s ⁻¹	[137]
Pd/CNFs	74.5	/	-0.541	-0.021	1 M/1 M/50 mV s ⁻¹	[138]
Pd/CNFs	66.1	1187	-0.511	-0.057	1 M/1 M/50 mV s ⁻¹	[139]
Pd/CNFs	80	1400	-0.46	-0.04	1 M/1 M/50 mV s ⁻¹	[140]
Pd-Ni/CNFs	200	/	-0.602	-0.072	1 M/1 M/10 mV s ⁻¹	[141]
Pd/SnO ₂ -GNS	46.1	/	-0.403	0.227	0.25 M/0.25 M/50 mV s ⁻¹	[142]
Pd-PANI	/	1300	-0.46	0.07	1 M/0.5 M/100 mV s ⁻¹	[56]
Pd/polyamide 6	70	/	/	-0.072	0.5 M/1.5 M/50 mV s ⁻¹	[143]
Pd/Nickel foam	107.7	/	-0.442	0.078	1 M/1 M/50 mV s ⁻¹	[144]
Pd-TiN	2.87	59.2	-0.474	0.022	0.5 M/1 M/20 mV s ⁻¹	[145]
Pd-NiO/MgO@C	69.3	/	-0.602	-0.052	1 M/1 M/10 mV s ⁻¹	[146]
Ru@PtPd/C	/	3600	-0.402	-0.052	1 M/1 M/30 mV s ⁻¹	[134]
Pd particles	151	/	-0.548	/	1 M/1 M/50 mV s ⁻¹	[147]
Nanoporous Pd	90.64	227.7	-0.403	0	0.5 M/1 M/10 mV s ⁻¹	[148]
Pd NWs	/	7.96 *	/	-0.01	0.5 M/1 M/50 mV s ⁻¹	[149]
Pd NWs	/	2.16 *	-0.566	-0.068	1 M/1 M/50 mV s ⁻¹	[150]
Pd/Au NWA	199	/	-0.402	0.138	1 M/1 M/50 mV s ⁻¹	[151]
PdPt	34	478	-0.523	0.077	1 M/1 M/50 mV s ⁻¹	[152]
Pd-Sn/C	121.59	/	-0.46	0.135	3 M/0.5 M/50 mV s ⁻¹	[153]
Pd-Ru-Sn/C	65	/	-0.536	0.097	3 M/0.5 M/50 mV s ⁻¹	[153]
Pd ₉₁ Sn ₉ /C	130	/	-0.205	0.347	1 M/1 M/50 mV s ⁻¹	[154]
Pd ₇ Ir/C	103	/	-0.584	0.008	1 M/1 M/50 mV s ⁻¹	[155]
Pd-Ni	6	/	/	-0.03	0.5 M/1 M/50mV s ⁻¹	[156]
Pd ₄₀ Ni ₆₀	180	/	-0.712	0.098	1 M/1 M/50mV s ⁻¹	[157]
Pd-Ni/CNF	199.8	/	-0.602	-0.072	1 M/1 M/10mV s ⁻¹	[131]
Pd-Ni-Zn/C	78.5	3600	-0.423	0.057	10 wt%/2 M/50mV s ⁻¹	[135]
Pd-Ni-Zn-P/C	108.7	3030	-0.373	0.097	10wt%/2 M/50 mV s ⁻¹	[135]
Pd-Ag/C	3.7**	/	-0.602	0.018	1 M/1 M/50mV s ⁻¹	[158]
Pd-Ag film	5 **	/	/	0.02	1 M/1 M/20 mV s ⁻¹	[159]
Pd-Pb/C	4.25 **	/	-0.452	-0.012	1 M/1 M/20 mV s ⁻¹	[160]
PdAu/C	165	/	-0.402	0.0273	1 M/1 M/50 mV s ⁻¹	[132]
Pd ₄ Au/C	/	/	0.5	0.88	1 M/0.25 M/10 mV s ⁻¹	[161]
Pd _{2.5} Sn/C	/	/	0.55	0.86	1 M/0.25 M/10 mV s ⁻¹	[161]
PdAu nanowire	83.7	/	-0.472	-0.001	1 M/1 M/50 mV s ⁻¹	[133]
Pd@Au/C	/	800	-0.41	0.04	1 M/1 M/50 mV s ⁻¹	[162]

* Unit: A·cm⁻²·mg⁻¹; ** This value was divided by the EASA.

4.1. Pd Supported on Carbon Materials

To improve the utilization efficiency of Pd, the commonly used catalysts are Pd nanoparticles loaded on supports. Various carbon materials such as carbon nanotubes, carbon nanospheres, carbon nanowires,

carbon nanofibers, porous carbon, fullerene and graphene have been used as the support. The supporting materials are required to have high surface area, low density, high chemical stability and excellent electrical conductivity.

4.1.1. Pd Supported on Carbon Spheres

In a series of work, Yan *et al.* [163–165] synthesized hollow carbon spheres/hemispheres and used them as catalyst support. The hollow carbon hemispheres (HCHs) provided high surface area (up to $1095.59 \text{ m}^2 \text{ g}^{-1}$) at reduced volume to improve the dispersion of the nanoparticles of the noble metal. At the same time, the hemispherical structure with hollow shell resulted in the improvement in the mass transfer, which leads to greatly improved stability. The peak current density of the ethanol oxidation on the Pd/carbon spheres catalyst reached almost four times higher than that of Pd/C catalyst. Figure 7 shows the typical results of the materials for the alcohol oxidation in alkaline solution. The catalyst showed the best performance for ethanol oxidation. It was revealed that on the same carbon support, the morphology of Pd greatly influenced the activity of ethanol oxidation, the Pd nanobars on carbon have much negative oxidation peak of ethanol than Pd particle on carbon [166].

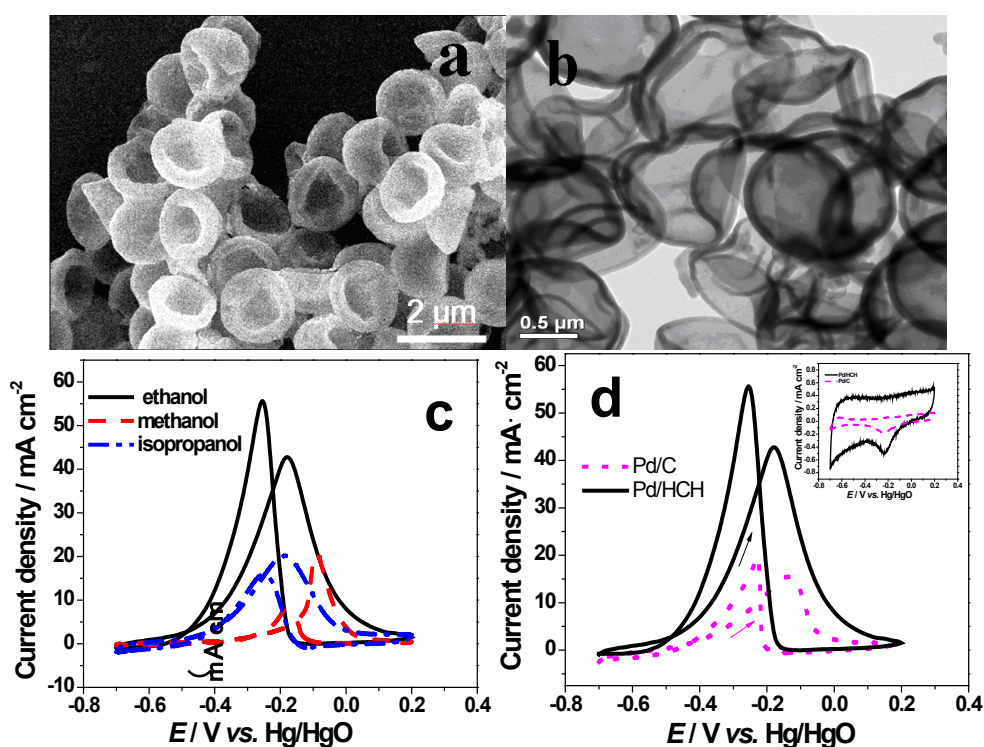


Figure 7. SEM microgram (a) and TEM image (b) of the HCHs with the mass ratio of PSs to glucose of 1:2 and the cyclic voltammograms of (c) different alcohol oxidation on Pd/HCH electrodes in $1.0 \text{ mol dm}^{-3} \text{ KOH}/1.0 \text{ mol dm}^{-3}$ alcohol solution at 303 K, scan rate: 50 mV s^{-1} and (d) ethanol oxidation on Pd/HCH and Pd/C electrodes in $1.0 \text{ mol dm}^{-3} \text{ KOH}/1.0 \text{ mol dm}^{-3}$ ethanol solution at 303 K, scan rate: 50 mV s^{-1} . The inset in Figure 7d is the cyclic voltammograms of Pd/HCH and Pd/C in $1.0 \text{ mol dm}^{-3} \text{ KOH}$ solution at 303 K, scan rate: 50 mV s^{-1} . Reproduced with permission from reference [130].

4.1.2. Pd Supported on Carbon Nanotubes

Carbon nanotubes (CNTs) can work as ideal substrate to modify the electrode surface used in electrochemistry. Immobilizing metal nanoparticles on CNTs has turned into an interesting field mainly due to the key role of CNTs and metal nanoparticles in the field of electrocatalysis. There are three typical methods for generating Pd nanoparticles on a CNTs surface: chemical reduction reaction, thermal decomposition and electrochemical reduction reaction. Chen *et al.* [136] synthesized Pd nanoparticles-carboxylic functional carbon nanotubes without surfactant. The material revealed high electrochemical activity and excellent catalytic characteristic for alcohol oxidation. Ding *et al.* [167,168] prepared Pd nanoparticles supported on multiwalled carbon nanotubes. Chu *et al.* [169] prepared Pd-In₂O₃/CNTs composite catalysts. The results showed that the addition of nanoparticles of In₂O₃ into Pd catalysts could significantly promote the catalytic activity for ethanol oxidation. Carbon nanotubes have higher graphitization degree than amorphous carbon which leads to higher stability in electrical environment, but higher graphitization also brings a drawback: it is not easy to load Pd nanoparticles on the surface of carbon nanotube evenly. The resolve of the dilemma will greatly accelerate the application of carbon naotube as catalyst support material in fuel cell.

4.1.3. Pd Supported on Carbon Nanofibers

Carbon nanofibers (CNFs) as a novel carbon material offered an ideal opportunity as catalyst support due to their superior electronic conductivity, anti-corrosion ability, and high surface area. Qin *et al.* [170–172] prepared Pd catalyst supported on carbon nanofibers (CNFs). The structure of the CNFs significantly affected the catalytic activity of the catalyst because the CNFs had high ratio of edge atoms to basal atoms and correspondingly faster electrode kinetics and stronger Pd-CNFs interaction. Maiyalagan *et al.* [131] prepared carbon nanofibers (CNF) supported Pd–Ni nanoparticles. The onset potential was 200 mV lower and the peak current density four times higher for ethanol oxidation for Pd–Ni/CNF compared to that for Pd/C. Cabon fibers prepared with novel nanotechnology can take the advantage of carbon nanotubes such as high graphitization and high surface area, at the same time it is also possible to construct functional groups on the surface of carbon fibers which is beneficial of the deposition of Pd nanoparticles, so carbon fiber will be a potential candidate as support material of Pd.

4.1.4. Pd Supported on Graphene

The combination of the high specific surface area (theoretical value of 2600 m² g⁻¹), excellent electronic conductivity, high chemical stability, unique graphitized basal plane structure and potentially low manufacturing cost, graphene nanosheets (GNS) can thus be exploited as an alternative material for catalyst support in fuel cells. Recently, graphene has received great attention as the catalyst support for fuel cell application. Wen *et al.* [173] prepared Tin oxide (SnO₂)/GNS composite as the catalyst support for direct ethanol fuel cells. Compared with Pd/GNS, the Pd/SnO₂-GNS catalyst showed superior electrocatalytic activity for ethanol oxidation. Chen *et al.* [174] prepared ultrafine Pd nanoparticles on graphene oxide (GO) surfaces. The as-made catalyst expressed high electrocatalytic ability in ethanol oxidation relative to a commercial Pd/C catalyst. Singh *et al.* [142] used graphene nanosheets (GNS) as

a catalyst support of palladium nanoparticles for the electrooxidation of ethanol. The Pd nanoparticles dispersed on GNS were more active compared to those dispersed on nanocarbon particles (NC) or multiwall carbon nanotubes (MWCNTs) for electrooxidation under similar experimental conditions. The enhanced electrochemical activity of Pd/GNS toward alcohol oxidation can be ascribed to the greatly enhanced electrochemical active surface area of Pd nanoparticles on the GNS support.

4.2. Pd Supported on Non-Carbon Supports

Conventional carbon supports are prone to undergo corrosion in aggressive electrolytes that are very often encountered in fuel cells. The corroded carbon support cannot hold the catalyst on its surface, leading to aggregation or sintering of noble metal particles (reduces electrochemical active surface area) and often resulting in oxidation and subsequent leaching of the catalyst. Corrosion of the support/catalyst happens mainly because they are exposed to aggressive electrolytes, high temperature and pressure, and high humidity. Carbon is known to undergo corrosion even at open circuit voltages of the fuel cell. So there are some attempts on the application of other materials other than carbon to use as support material of Pd.

4.2.1. Pd Supported on Conducting Polymers

Polyaniline (PANI) is one of the most important conducting polymers remarkable for its high stability, solution processability and tunable electrical conductivity, which can be controlled by simple doping of the polymer. Pandey *et al.* [56] deposited a porous Pd-polyaniline (Pd-PANI) nanofiber film on conducting surfaces and the Pd-PANI showed excellent electrocatalytic activity towards the oxidation of ethanol. Su *et al.* [143] prepared Pd/polyamide 6 (Pd/PA6) nanofibers with high surface area using a simple electroless plating method. The Pd/PA6 showed excellent mechanical property, good conductivity, and high porosity. The large surface area and reduced diffusion resistance of the free-standing Pd/PA6 nanofibers led to a superior catalytic property.

4.2.2. Pd Supported on Zeolite

Zeolite has a large specific area with strongly organized microporous channel systems in which both a regular and high dispersion of metal nanoparticles can be obtained. El-Shafei *et al.* [175] prepared Pd-zeolite graphite (Pd-ZG) electrodes for ethanol oxidation. The Pd-ZG electrodes showed a better activity as well as poisoning tolerance during ethanol oxidation in alkaline medium in comparison with Pd electrode.

4.2.3. Pd Supported on Metal Supports

Nickel foam has the advantages of extinguished electronic conductivity, low weight, and 3-D cross-linked grid structure which provides high porosity and surface area. It can be used as an ideal support of catalyst. The nickel foam would not only reduce the diffusion resistance of the electrolyte but also enhance the facility of ion transportation and maintain the very smooth electron pathways in the rapid electrochemical reactions. Wang *et al.* [144] fabricated a three-dimensional, hierarchically structured Pd electrode by direct electrodeposition. The improved electrocatalytic activity and

excellent stability of the Pd/Nickel foam electrode make it a favorable platform for direct ethanol fuel cell applications.

Metal nanowire or nanotube array architecture can be a potential substrate to improve noble metal utilization efficiency [176]. Besides it can act as a template, which means that no stabilizer is required, it also serves as an excellent current collector. Cherevko *et al.* [151] prepared highly ordered Pd decorated Au nanowire arrays (Pd/Au NWA). The maximum current densities were several times higher on the modified electrodes than on the unmodified Pd NWA. The highly active electrode showed almost 4-fold increase in the peak current for ethanol oxidation. The synergistic effect between substrate and deposited materials was a most important factor infusing such unusually high activity.

4.2.4. Pd Supported on Nitrides

Titanium nitride (TiN) is a very hard, conducting ceramic material used as an abrasive coating for engineering components. It possesses metal-like electronic conductivity with a very reproducible surface for electron transfer. Thotiyl *et al.* [145] studied the excellent metal-support interaction between Pd and TiN and found the efficient ethanol oxidation coupled with excellent stability of the Pd-TiN catalyst.

4.3. Performance of Pd Novel Nano Structures

4.3.1. Core-Shell Structure

Hybrid nanomaterials, particularly, the core-shell structured hybrid nanomaterials are promising due to their multi-functional and designable properties. The core/shell structured nanomaterials has the ability to improve the stability and surface chemistry of the core materials. It is possible to obtain unique structures and properties for applications via a combination of the different characteristics of the components that are not available with their single-component counterparts. The carbon-coated nanomaterials are of great interest due to their stability toward oxidation and degradation [177]. The creation of the core/shell nanostructures containing bi-metal oxides greatly enhanced the catalytic efficiency of these structures over pure single metal oxide particles [178]. Mahendiran *et al.* [146] synthesized carbon coated NiO/MgO in a core/shell nanostructure. The results indicated that the Pd-NiO/MgO@C catalyst has excellent electrocatalytic activity and stability. Gao *et al.* [134] synthesized a core-shell structured Ru@PtPd/C catalyst, with PtPd on the surface and a Ru as core. The ethanol oxidation activities of the Ru@PtPd/C catalysts were 1.3, 3, 1.4 and 2.0 times as high as that of PtPd/C, PtRu/C, Pd/C and Pt/C with same PtPd loadings, respectively. The stability of the Ru@PtPd/C was higher than that of Pt/C and PtPd/C. Ksar *et al.* [38] synthesized bimetallic Pd-Au nanostructures with a core rich in gold and a Pd porous shell. The Pd shell-Au core nanostructures synthesized in mesophases were promising for application in direct ethanol fuel cells as they exhibited a very good electrocatalytic activity and a high stability. The core-shell structure has some essential advantages such as the synergistic effect between the core material and the shell which can improve the kinetics of the reaction, the porous structure which greatly improves the mass transfer in the electrode and the reduced cost because of the less use of the noble metal. So vast efforts have been

devoted to this field, but the core-shell structure is limited by the preparation technique and its application in the membrane electrode assembly of fuel cell is still a challenge.

4.3.2. Other Structures

Yu *et al.* [28] prepared dendritic Pd nanostructures, which exhibited high catalytic activity toward ethanol oxidation in alkaline media. Yin *et al.* [147] prepared Pd nanoparticles and the ethanol oxidation on the Pd catalysts took place at a more negative anodic potential, implying a reduced overpotential. Wang *et al.* [148] fabricated nanoporous Pd composites through chemical dealloying of the Al₇₀Pd₃₀ alloy. The nanoporous Pd composites had high electrochemical active surface areas and exhibited remarkable catalytic activities toward ethanol oxidation in alkaline media. Liu *et al.* [149] synthesized Pd nanowires with high catalytic activity and long-term stability toward the oxidation of alcohols. Ksar *et al.* [150] synthesized Pd nanowires with length of a few tens of nanometers. The Pd nanowires exhibited both a very important catalytic activity for ethanol oxidation and a very high stability. Liu *et al.* [31] prepared raspberry hollow Pd nanospheres (HPNs)-decorated carbon nanotube (CNT) for the oxidation of ethanol in alkaline media. The catalyst was fabricated by attaching HPNs onto the surface of the functionalized CNT. The hybrid nanostructure exhibited higher mass activity toward ethanol oxidation which increased the utilization of Pd. Pd dendritic structure, Pd nanowires, hollow raspberry spheres, hollow spheres [179], nanoparticles and nanomembrane [180] are prepared and all showed superior catalytic activity in ethanol oxidation, but they share the same problem with the core-shell structure: how to a material with high half-cell performance into a material with high full cell performance, which still needs great efforts in the preparation technique.

4.4. Pd Alloys

Pd is well known to be very active for ethanol oxidation in alkaline. Alloying Pd with another metal M (M = Au, Sn, Ru, Ag, Ni, Pb and Cu) is expected to increase the activity and at the same time the stability of the catalyst for the EOR in alkaline media [181].

4.4.1. PdNi Alloys

Qiu *et al.* [156] prepared bimetallic Pd-Ni thin film on glass carbon electrodes (GCEs). The high catalytic activity and the low cost of the Pd-Ni films enable them to be promising catalyst for the oxidation of methanol and ethanol in alkaline media. Qi *et al.* [157] fabricated Pd₄₀Ni₆₀ alloy catalyst with an enhanced catalytic performance toward ethanol oxidation in alkaline media compared with nanoporous Pd. Maiyalagan *et al.* [131] prepared carbon nanofibers (CNF) supported Pd-Ni nanoparticles. The onset potential was 200 mV lower and the peak current density was four times higher for ethanol oxidation on Pd-Ni/CNF compared with that of Pd/C. Shen *et al.* [182] synthesized carbon-supported PdNi catalysts for the ethanol oxidation reaction in alkaline direct ethanol fuel cells. The Pd₂Ni₃/C catalyst exhibited higher activity and stability for the EOR in an alkaline medium than that on Pd/C catalyst. Bambagioni *et al.* [135] prepared Pd-(Ni-Zn)/C and Pd-(Ni-Zn-P)/C catalysts which provided excellent results in terms of the specific current and onset potential at room temperature.

4.4.2. PdAu Alloys

Xu *et al.* [132] prepare Pd-Au alloy catalyst for the EOR in an alkaline medium. The catalyst samples were in sequence of Pd/C > Pd₃Au/C > Pd₇Au/C > PdAu/C in terms of the peak current density. However, the stability tests demonstrated that the catalyst samples were in sequence of PdAu/C > Pd₃Au/C > Pd₇Au/C > Pd/C. Cheng *et al.* [133] prepared highly ordered PdAu nanowire arrays (NWAs). The onset potential of ethanol oxidation on the PdAuNWAs electrode was 123 mV more negative compared with that on the Pd NWAs due to the synergistic effect of Pd-Au bimetallic alloy. He *et al.* [161] prepared carbon-supported Pd₄Au and Pd_{2.5}Sn-alloyed nanoparticles, the results suggested that the Pd-based alloy catalysts represented promising candidates for the oxidation of ethanol. The Pd₄Au/C displayed the best catalytic activity among the series for the ethanol oxidation in alkaline media. Zhu *et al.* [162] decorated carbon-supported gold nanoparticles with mono- or sub-monolayer Pd atoms, the Pd@Au/C had higher specific activities than that of Pd/C for the oxidation of ethanol in alkaline media. This suggested that the Pd utilization was improved with such a surface-alloyed nanostructure. Several other alloys such as the PdPt alloy [152,183–185],

PdSn alloy [153,186], PdIr alloy [155,187], PdAg alloy [158,159,188], PdTi alloy [189] and PdPb alloy [160] were also studied as the catalysts for the EOR.

4.5. Single Fuel Cell Characterizations

Although there were quite a lot reports about the Pd-based catalysts for ethanol oxidation, especially, in alkaline media, the performance of a direct ethanol fuel cell operating in alkaline membrane was rarely reported. The reason is that the anion-exchange membrane is not commercially available. The Tokuyama company in Japan is one of the pioneers in the anion-exchange membrane and most reported work were using their membranes. In recent years, Zhao's group [132,182,190,191] has done most of the work on the anion-exchange membrane direct ethanol fuel cells (AEMDEFCs). Other researchers such as Antolini [192] and Bambagioni [193] also tested the performance of the AEMDEFC, the results of these groups were compared in Figure 8. It is found that the PdNi alloy had the highest activity which was in accordance with the half cell testing. Among all catalysts, the Pd/C had the lowest activity. The change of carbon powders to carbon nanotubes improved the performance. A promising way was to alloy Pd with other metals, especially, with Ni. The highest activity of the PdNi alloy catalyst reached more than 3 times higher than that of Pd/C catalyst. The conclusion is similar with the half-cell results: alloying with other metals will improve the performance, attention should be put to multi-alloys. Another conclusion reached is the advantage of carbon nanotube *versus* carbon powder with enhanced performance.

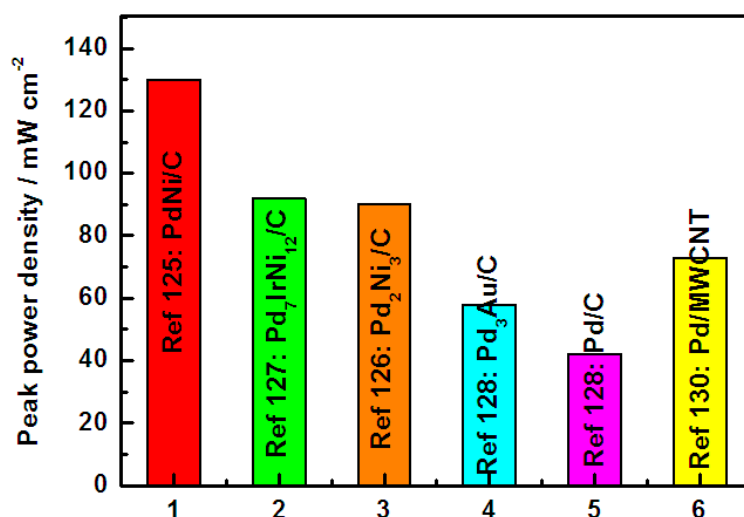


Figure 8. Peak powder density of single fuel cell performance of the Pd catalysts in anion-exchange membrane direct ethanol fuel cells (AEMDFECs).

5. Pd-Based Catalysts for the Oxygen Reduction Reaction (ORR)

Oxygen reduction reaction (ORR) is one of the important catalytic reactions due to its role in metal corrosion and electrochemical energy converters and, in particularly, fuel cells. Pt group metal based catalysts were currently used for PEMFCs to reduce the large ORR overpotential. Unfortunately, even on the most active Pt surface, the overpotential was over 250 mV at open circuit voltage (OCV). The thermodynamic efficiency dropped from 83% (1.229 V) to 66% at an OCV value of 0.98 V under standard conditions. Since the exchange current density of the ORR is several orders of magnitude slower than that of the hydrogen oxidation reaction (HOR) (10^{-9} A cm⁻² vs. 10^{-3} A cm⁻²), the operating voltage must be largely reduced to about 0.65 V at a reasonable current density, making the electronic efficiency of the PEMFCs only at 44% [194]. Pt is widely used as the catalyst for ORR due to its high activity and excellent chemical stability. However, Pt is expensive and the limited supply of Pt poses serious problems to widespread commercialization of the fuel cell technology. Thus, research efforts in the development of cathode catalyst have been focused on decreasing the Pt content or replacing it with less expensive materials while maintaining high ORR activity. An alternative approach is to replace Pt with less expensive, catalytically active, and relatively stable noble metals and to alloy the noble metals with base metals to enhance their stability and activity via electronic modification. Pd is the second most active metal for the ORR. Pd possesses a similar valence electronic configuration and lattice constant to Pt and highly methanol-tolerant ability. However its mass activity for the ORR is approximately five times lower than that of Pt. In an acidic electrolyte, the exchange current density of Pd for ORR is 10^{-10} A cm⁻², which is one magnitude lower than that of Pt (10^{-9} A cm⁻²). Binary Pd-base metal (BM) (where BM = Co, Ni, Fe, Cu, W and Mo) systems have been identified as promising PEFC cathode catalyst with enhanced activity for ORR and stability compared to Pd alone. The origin of the enhanced activity has been linked to the modification of the electronic structure of Pd upon bonding with the alloying metal. In addition to enhancing activity, the dissolution potentials of the noble metals may be shifted to higher potentials, stabilizing the catalyst against dissolution in acidic medium.

With the rapid development of alkaline anion exchange membranes for substituting the conventional aqueous alkaline electrolyte, attention has been drawn to the study of ORR catalysts in alkaline media. More ORR catalysts are available for operation in alkaline than in acidic media due to the excessive corrosion in acidic solutions. In alkaline solution, Pd-based alloys are suitable alternative of Pt not only due to its lower costs and more abundance but also to the lower activity for the adsorption and oxidation of methanol in direct methanol fuel cells which tends to crossover to the cathode compartment and inhibits ORR. Recent reports have shown that ORR activity on the Pd alloys is comparable or slightly better than that on Pt/C.

Table 3 summarized the performance of Pd and Pd alloys as catalysts for ORR. In acidic solution, the most positive onset potential on Pd catalyst was only 0.87 V vs. RHE which was almost 0.2 V negative compared with Pt catalyst. In alkaline solution, the onset potential on Pd catalyst was comparable to that of Pt catalyst. The onset potential could be improved to 1.05 V when alloyed with Pt, the highest record for alloying with non-noble metal was 0.96 V in half cell testing. Fuel cell testing gave similar conclusions. The performance of Pd catalyst could not surpass that of Pt catalyst in both PEMFC and direct alcohol fuel cells, but when Pd was alloyed the performance could be slightly better than or comparable to the commercial Pt catalyst.

Table 3. Comparison of the onset potential and mass activity of Pd for oxygen reduction reaction (ORR).

Catalysts	Mass Activity/ $\text{mA mg}^{-1}\text{Pd}$	Onset Potential/V vs.	Conditions Solution **/Scan	References
		RHE	Rate/Rotating Speed	
Pd/C	/	0.87	A/5 mV s^{-1} /1600 rpm	[195]
Pt/C (JM)	/	1.05	A/5 mV s^{-1} /1600 rpm	[195]
Pd-PPy/C	/	0.82 (NHE)	A/5 mV s^{-1} /1600 rpm	[196]
40% E-TEK Pt/C	/	0.98 (NHE)	A/5 mV s^{-1} /1600 rpm	[196]
Pd/Vulcan XC-72R	47 at 0.7 V *	0.82	A/5 mV s^{-1} /1600 rpm	[197]
20% E-TEK Pt/C	/	0.92	A/5 mV s^{-1} /1600 rpm	[197]
E-Tek 20% Pd/C	23 at 0.7 V *	0.77	A/5 mV s^{-1} /1600 rpm	[197]
PdFe-WC/C	/	0.91	A/10 mV s^{-1} /1600 rpm	[198]
Pt ₅₀ Au ₅₀ /Ce _x C	4.1 at 0.7 V *	/	A/5 mV s^{-1} /1600 rpm	[180]
PdCoMo/CDX975	4.1 at 0.7 V *	0.915	A/5 mV s^{-1} /1600 rpm	[199]
Pd/CDX975	1.6 at 0.7 V *	0.84	A/5 mV s^{-1} /1600 rpm	[199]
Pd _{100-x} W _x	/	0.85	A/5 mV s^{-1} /1600 rpm	[200]
Pd	/	0.7	A/5 mV s^{-1} /1600 rpm	[200]
PdPt/C	/	0.98	A/5 mV s^{-1} /1600 rpm	[201]
Pt rich-core Pd rich-shell	9 at 0.85 V * (catalyst)	/	A/5 mV s^{-1} /1600 rpm	[202]
JM20 Pt/C	5.8 at 0.85 V * (catalyst)	/	A/5 mV s^{-1} /1600 rpm	[202]
Pd/Au	0.34 at 0.8 V *	/	A/10 mV s^{-1}	[203]
	1.1 at 0.8 V *	/	B/10 mV s^{-1}	[203]
Pd/MWCNTs	/	0.76 (SHE)	B/10 mV s^{-1}	[91]
PdCu/C	23 at 0.9 V *	0.96	B/10 mV s^{-1} /1600 rpm	[204]
Pd-Cu film	/	0.86	B/5 mV s^{-1} /1000 rpm	[205]
Pd-Co/C	3.6 at 0.7 V *	/	B/5 mV s^{-1} /1600 rpm	[206]
Pt-Pd/C	/	0.92	B/5 mV s^{-1} /1600 rpm	[207]

Table 3. Cont.

Catalysts	Mass Activity/ $\text{mA mg}^{-1}\text{Pd}$	Onset Potential/V vs.	Conditions Solution **/Scan	References
		RHE	Rate/Rotating Speed	
Pt–Pd/C	114.87 at 0.9 V * (Pt)	1.05	B/5 mV s^{-1} /1600 rpm	[208]
Pt/C	73.87 at 0.9 V * (Pt)	1.0	B/5 mV s^{-1} /1600 rpm	[208]
PdFe@PdPt/C	1.92 at 0.8 V * (Pt)	/	B/20 mV s^{-1} /1600 rpm	[209]
	1.2 at 0.8 V * (Pt)	/	B/20 mV s^{-1} /1600 rpm	[209]
PdCo@PdPt/C	65 at 0.9 V * (Pt)	/	B/20 mV s^{-1} /1600 rpm	[210]
	14 at 0.9 V * (Pt)	/	B/20 mV s^{-1} /1600 rpm	[210]
PdFe Nanorods	284 at 0.85 V *	/	B/10 mV s^{-1} /1600 rpm	[211]
	265 at 0.85 V * (Pt)	/	B/10 mV s^{-1} /1600 rpm	[211]
Pt/Pd/Pd3Fe	1.8 at 0.9 V *	/	B/20 mV s^{-1} /1600 rpm	[212]
Pt(111)	0.8 at 0.9 V *	/	B/20 mV s^{-1} /1600 rpm	[212]
Pd/SnO ₂ –KB	0.75 at 0.8 V *	0.88	B/5 mV s^{-1} /900 rpm	[64]
Pd/KB	0.28 at 0.8 V *	0.86	B/5 mV s^{-1} /900 rpm	[213]
Tanaka Pt/C	/	0.95	B/5 mV s^{-1} /900 rpm	[213]
Pd/GNS	280 at 0.9 V *	1.06	C/10 mV s^{-1} /1600 rpm	[188]
Pt/GNS	110 at 0.9 V *	1.0	C/10 mV s^{-1} /1600 rpm	[188]
Pd@MnO ₂ /C	450 at 0.9 V *	1.02	D/10 mV s^{-1} /2500 rpm	[214]
Pd black	180 at 0.9 V *	1.07	D/10 mV s^{-1} /2500 rpm	[214]

* The potentials were vs. RHE; **solution A: 0.5 M H₂SO₄, solution B: 0.1 M HClO₄, solution C: 0.1 M NaOH and solution D: 0.1 M KOH.

5.1. Pd Supported on Carbon Materials

5.1.1. Pd on Carbon Powder

Although Pd is the second most active metal for the ORR, its mass activity is approximately five times lower than that of Pt since the ORR exchange current density is one magnitude lower than that of Pt. Tang *et al.* [195] synthesized a carbon supported Pd/C catalyst which showed high activity for the ORR. However, the performance of the Pd/C was still much poorer than that of the commercial Pt/C. There was a big difference in onset potential for the ORR in acidic solution. Single cell with Pd/C as the cathode displayed a maximum power density of 508 mW cm^{-2} , which was almost half of that of the commercial Pt/C catalyst. Different supporting materials such as highly ordered pyrolytic graphite and modified carbon was studied [215]. Jeyabharathi *et al.* [196] synthesized carbon-supported Pd-polypyrrole (Pd-PPy/C) nanocomposite. The introduction of Pd in the conducting PPy/C matrix gave higher catalytic activity toward ORR with resistance to methanol oxidation. The performance of the Pd-PPy/C catalyst was still inferior to the Pt/C catalyst. Kumar *et al.* [197] studied the influence of the chemical pretreatment of carbon support for ORR on Pd nanoparticles in acidic electrolyte. They found that the chemical treatment significantly changed the surface chemical properties and surface area of the carbon support. The kinetics of ORR on these catalysts predominantly involved a four-electron step. The performance of the Pd on pretreated carbon support was found to be much higher than the commercial E-Tek 20% Pd/C catalyst with the mass activity of $47 \text{ mA mg}^{-1}\text{Pd}$ at 0.7 V RHE compared to $23 \text{ mA mg}^{-1}\text{Pd}$ of E-Tek catalyst. It is concluded that limited by the intrinsic kinetic of ORR

on different metals, the performance of the most popular Pd/C catalyst is much less than the Pt/C catalyst. However, considering the difference in the cost, it is still meaningful to study the Pd/C catalyst, but new material or structure should be put more attention.

5.1.2. Pd Supported on Carbon Nanotubes

Chakraborty *et al.* [91] synthesized nanosized Pd particles supported on multiwalled carbon nanotubes (MWCNTs). The authors concluded that the catalytic reduction of the oxygen followed a four electron pathway on Pd-based catalysts. Jukk *et al.* [216] found enhanced electrocatalytic activity of PdNP/MWCNT modified GC electrodes and the oxygen electroreduction kinetics were higher compared with those of bulk palladium electrodes. The number of electrons transferred per oxygen molecule was calculated to be 4. Kim *et al.* [217] studied the influence of counter ions on the oxygen reduction of Pd catalyst on functionalized carbon nanotube and found that the electrocatalytic activity is affected by the nature of anion of imidazolium salt. As is known the activity of Pd on carbon powder is less than Pt/C, not too much work is done on the attempts of loading Pd on carbon nanotubes for ORR application. However if carbon nanotubes can be helpful in the stability there will be new interest in this field.

5.1.3. Pd Supported on Graphene

Graphene is found to have vast applications in many fields where carbon powder or carbon nanotubes are used, for example as catalyst support in electrocatalysis. There was no report to prove that the activity of Pd catalyst for the ORR could surpass that of Pt catalyst in acidic solution. However, it is possible for the Pd catalyst to perform better than that of the Pt catalyst for the ORR in alkaline solution when supported on graphene. Seo *et al.* [218] studied graphene supported Pd catalyst in alkaline media. The graphene-supported Pd catalyst (Pd/GNS) showed significantly high catalytic activity for the ORR with higher mass activity and surface area for ORR in an alkaline solution. The catalyst was more favorable for ORR than that of the Pt/GNS catalyst at high metal loadings. The mass activity at 0.85 V vs. RHE of the Pd/GNS reached $0.84 \text{ mA } \mu\text{g}^{-1}\text{Pd}$, while, the value was $0.35 \text{ mA } \mu\text{g}^{-1}\text{Pd}$ for the Pt/GNS. Pd metal decorated graphene oxide was found to have high ORR activity via the direct four electron pathway [219]. Gotoh *et al.* [220,221] also proved that Pd supported on graphene oxide showed better performance in ORR than Pt.

5.2. Pd Supported on Oxides

Oxides such as manganese dioxide was used as support to form Pd@MnO₂ catalyst [214]. The ORR onset potential on the Pd@MnO₂ catalyst positively shifted for more than 250 mV compared with the MnO₂ catalyst without Pd. Both the ORR onset potential and the limit current density obtained by the rotating disk electrode (RDE) measurements on the Pd@MnO₂ catalyst were close to those on the Pd black catalyst. The mass activity of the Pd@MnO₂ catalysts (normalized by Pd mass) was 2.5 times higher than that of the Pd black catalyst. The PtPd/TiO₂ electrocatalyst with a proper ratio of Pt/Pd showed activity comparable to that of a commercial Pt/C catalyst [222]. The interaction between Pd and

highly dispersed TiO₂ is proven to improve the catalytic activity of Pd supported on TiO₂-modified carbons [223].

5.3. Pd Alloys

The intrinsic catalytic activity of Pd for the ORR is lower than that of Pt and the long-term stability at high potentials is also not as good as that of Pt. It has been proven that the ORR takes place on Pd in the same manner as that on Pt. As like Pt, the oxygen intermediate species will be covered on Pd surface at technically relevant potentials regioning from 0.7 to 0.9 V vs. NHE and hinders oxygen reduction. So the development of the Pd alloy catalysts that inhibit the adsorption of oxy/hydroxy species and enhance the ORR activity has been of interest. Bimetallic catalysts often exhibit notably different catalytic and chemical properties than their corresponding monometallic component. Bimetallic systems often provide enhanced selectivity, stability, and/or activity [224,225]. Several mechanisms to explain the catalytic properties of bimetallic catalysts have been proposed including geometric or ensemble effects, formation of bifunctional surfaces and electronic modification of the surface sites [226].

5.3.1. PdFe Alloys

Yin *et al.* [198] synthesized a PdFe-WC/C cathodic catalyst for ORR. The ORR activity of the PdFe-WC/C catalyst in acidic solution was found to be comparable to that of Pt/C catalyst. It was believed that the high catalytic activity as a Pt-free catalyst originated from the synergistic effect between PdFe and WC. The alcohol-tolerance and selectivity of the PdFe-WC/C catalyst are favorable for the ORR. Tungsten-based materials as novel supports have been intensively studied due to their chemical and/or electrochemical activities for various reactions as they exhibit a synergistic effect in many reactions. The use of WC as the catalyst support for PEMFCs and DMFCs has also been reported [227–231] PdFe/C catalyst was also found to have better performance in ORR than Pd/C catalyst [232,233].

5.3.2. PdCu Alloys

Gobal *et al.* [234,235] prepared CuPd alloys with different compositions on nickel. The number of transferred electrons involved in the ORR on Pd-Cu alloys is four, which is the same as Pt. A 60 mV/dec Tafel slope for the ORR was found for all the PdCu alloys. The enhancement of the activity of the alloy toward ORR was attributed to the change in geometric and electronic structures of Pd caused by the insertion of Cu. Kariuki *et al.* [204] prepared monodispersed PdCu alloy nanoparticles, which showed high ORR activity in acidic electrolyte. Fouda-Onana *et al.* [205] found Pd₅₀Cu₅₀ exhibited the high activity in ORR. The enhancement was attributed to an optimal *d*-band property that made the OOH dissociative adsorption easier, which was considered as chemical rate determining step (RDS) for the ORR [236,237].

5.3.3. PdAg Alloys

Ag catalysts have lower activity in ORR than those of Pt catalysts because of their weak interaction for binding O₂. However, the inexpensive Ag nanoparticles have been shown to have higher stability

than pure Pt cathodes during long-term operation. Lee *et al.* [238] supported AgPd alloy on multiwalled carbon nanotubes and found that the ORR proceeded through a two-electron pathway, while according to other authors the ORR on AgPd alloy was a four-electron process [239,240]. In alkaline medium the electrode reaction kinetics is higher than that in the acidic medium, enabling the use of Pt-free catalysts. Oliveira *et al.* [159] evaluated PdAg alloys toward the ORR in alkaline medium and found that alloying Pd with Ag led to an increase in the ORR kinetics relative to Pd.

5.3.4. PdAu Alloys

Gold has been used as support material for studying the catalytic behaviour of Pd. Sarapuu *et al.* [203] evaluated the influence of the Pd film thickness and Au substrate to the ORR activity of Pd. The ORR proceeded through 4-electron pathway on all PdAu electrodes. The specific activity of ORR was lower in H₂SO₄ solution and decreased slightly with decreasing the Pd film thickness. In HClO₄, the specific activity was higher and was not significantly dependent on the film thickness. Xu *et al.* [241] found Au-modified Pd catalyst exhibited increased catalytic activity for ORR in alkaline media, which was 1.4 times higher than that with the mono-Pd catalyst.

5.3.5. PdCo Alloys

There was an in-depth understanding of the various factors that influence the catalytic activity of the PdCo nanoalloys [242–244]. It was found that a mild annealing of the alloys at moderate temperatures (350 °C) was desirable to clean the surface and maximize the catalytic activity and durability [245–247]. Tominaka *et al.* [248] synthesized a mesoporous PdCo sponge-like nanostructure with a most desirable lattice contraction into a Pd catalyst for the ORR. The mesoporous PdCo catalyst had a higher specific activity than that of the Pt catalyst. Wei *et al.* [206] obtained PdCo/C alloy catalysts with an atomic ratio of 3:1. They found the well-formed PdCo alloy showed excellent ORR activity. Serov *et al.* [249] investigated PdCo catalysts for ORR in a direct methanol fuel cell. Such a non-Pt catalyst showed comparable power density with a commercial MEA prepared using Pt cathode. Rao *et al.* [199] prepared PdCoMo alloy nanoparticles with better catalytic activity compared with Pd.

5.3.6. PdPt Alloys

The nanosized Pd supported on carbon black will gradually grow larger during long-term operation, thus reducing the electrochemical active surface area and resulting in irreversible performance loss. Many works had been tried to improve the performance and durability of the catalyst, alloying with other metal is one important method. Lots of works had been done on the alloys of Pd with other noble metal, for example Pt [250–252]. Pd and Pt had a face-centered cubic (fcc) phase with a unit length of 3.92 Å for Pt and 3.89 Å for Pd. The small lattice mismatch meant that the epitaxial growth should be favored. Figure 9 shows a typical result of PdPt alloy for the ORR. The PdPt nanodendrites were two and a half times more active than the state-of-the-art Pt/C catalyst [253–255].

The PtPd/C showed a comparable performance and better durability than that of the Pt/C [201]. Thanasilp *et al.* [256] demonstrated that the different Pt:Pd atomic ratios had a significant effect on the catalyst activity. Decreasing the Pt:Pd atomic ratio led to an increase in the particle size and decrease

in the electrochemical activity. Fıçıcılar *et al.* [257] found that when the particle size of Pd increased with the content and a lower Pd content exhibited a considerable activity and increased stability. Chang *et al.* [202] found that the Pt₃Pd₁/C nanocatalyst has a 50% enhancement in ORR due to the synergistic effect. Ohashi *et al.* [207] prepared various PtPd/C bimetallic catalysts with a higher tolerance to ripening induced by potential cycling. Peng *et al.* [208] designed a Pt particle-on-Pd structure to address both the activity and stability issues. Other alloys of Pd–W, [200] Pd–V, [258] Pd–Ni [259,260], Pd–Sn [261,262] and Pt–Ir–Re [263] were also studied as catalysts for the ORR.

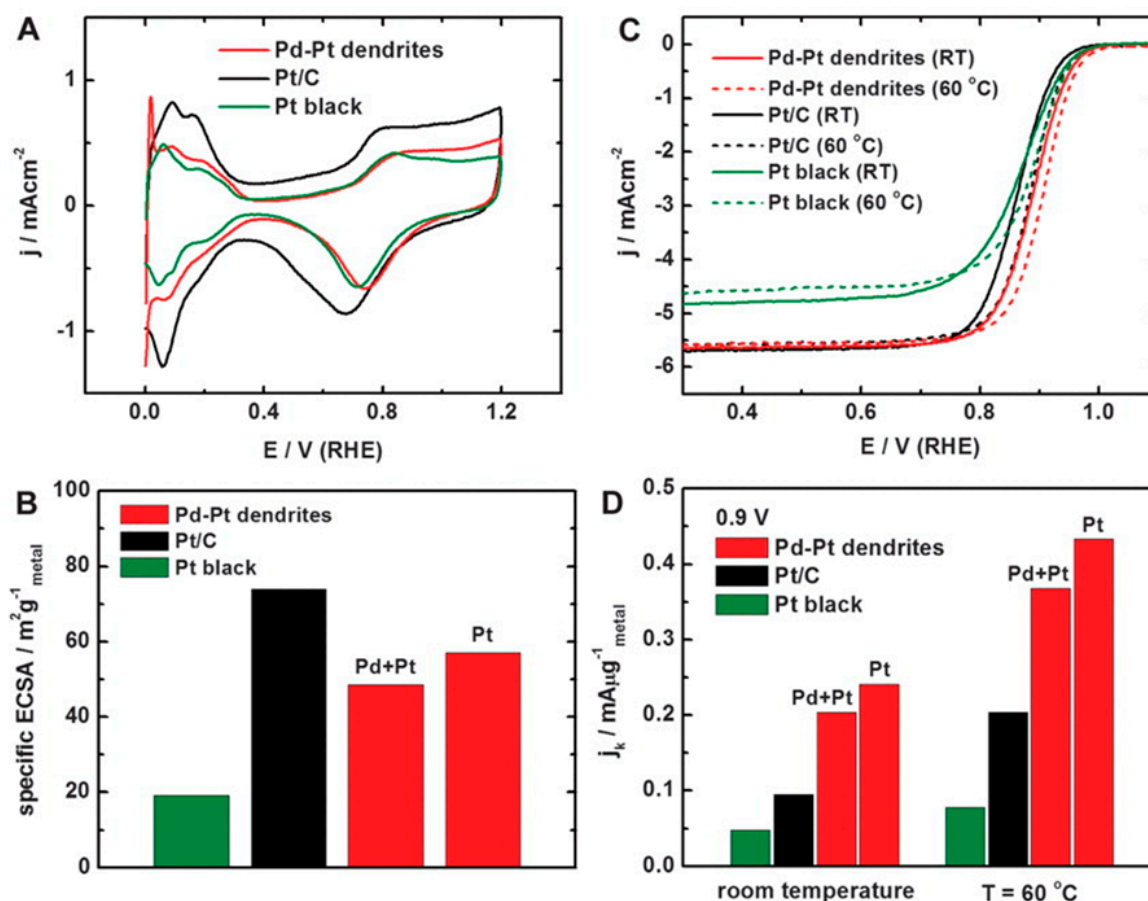


Figure 9. Comparison of the catalytic properties of the Pd-Pt nanodendrites, Pt/C catalyst (E-Tek), and Pt black (Aldrich). (A) The CV curves recorded at room temperature in an Ar-purged 0.1 M HClO₄ solution with a sweep rate of 50 mV s⁻¹; (B) specific ECSAs (electrochemical active surface area) for the Pd-Pt nanodendrites, Pt/C catalyst, and Pt black; (C) ORR polarization curves for the Pd-Pt nanodendrites, Pt/C catalyst and Pt black recorded at room temperature and 60 °C in an O₂-saturated 0.1 M HClO₄ solution with a sweep rate of 10 mV s⁻¹ and a rotation rate of 1600 rpm and (D) mass activity at 0.9 V versus RHE (reversible hydrogen electrode) for these three catalysts. Reproduced with permission from reference [253].

5.4. Novel Nanostructures

Recent attention has been drawn to the strong dependence of the catalytic properties of Pd on their surface morphologies. For example, the specific activity of the Pd nanorods prepared by

electrodeposition was found to be close to that of Pt in acidic solution and was 10 times higher than that of electrodeposited Pd nanoparticles [264]. The higher activity was attributed to the exposure of Pd (110) surface facet. The activity of the Pd with low index planes increased in the following order: Pd(110) < Pd(111) < Pd(100) [265–267]. The Pd(100) single crystal plane was even more active than Pt(110) in 0.1 M HClO₄. The low indexed Pd became favorable in the electrochemical reaction, controlling the morphology is one of the commonly used methods to get low indexed metal.

5.4.1. Core-Shell Structures

The heterogeneous core shell structure has many advantages. First of all, the core-shell structure can greatly reduce the cost of the catalyst. Second, the strain caused by the lattice mismatch between the surface and core components may be used to modify the electronic properties of the surface metal atoms, most notably their *d*-band centres, which affect the rates of one or more elementary steps in the overall catalytic reaction [268–270].

Lim *et al.* [253] synthesized PdPt bimetallic nanodendrites consisting of Pt branches as shell and Pd as core, the nanodendrites were two and half times more active for the ORR than the state-of-the-art Pt/C catalyst. Peng *et al.* [208] also found improved stability for ORR with a Pt-on-Pd core-shell nanostructure. It was calculated that the optimal coverage of Pt on Pd (111) surface was on the order of two monolayers [271]. Yang *et al.* [209] prepared a core-shell structure with a PdFe core and a PdPt shell, which showed four times ORR activity compared with a commercial Pt/C catalyst. Yang *et al.* [210] constructed a PdPt shell on a PdCo core with six fold increases in the activity and with much higher stability. Sasaki *et al.* [272] illustrated a core/shell catalyst with Pd and Pd₉Au₁ alloy as core and Pt monolayer as shell with high activity and very high stability. The origin of the improved activity and stability of the core-shell catalyst was studied. The Pd core not only assured the long-term stability of the monolayer Pt shell, but increased the activity of Pt by causing it to contract slightly, lowering its *d*-band centre energy and reducing the bond strength of the adsorbed oxygen intermediates. These effects decreased the bonding of OH and O to Pt that inhibited the ORR kinetics and also stabilize Pt against oxidation and dissolution.

5.4.2. Unsupported Pd

Besides the most frequently used supported Pd catalysts, the application of nano-structured Pd as catalyst for the ORR has also been studied. For example, PdFe nanorods [211], PdCo_xCN_y [273], Pt monolayer supported on Pd/Pd₃Fe [212] and Pd/SnO₂ [213] demonstrated significantly increased ORR activity. The catalytic activity of Pd could become comparable to that of Pt upon appropriate modification of its electronic structure. The surface specific activity of Pd nanorods (Pd-NRs) toward the ORR was found to be not only 10-fold higher than that of Pd nanoparticles (Pd-NPs), but also comparable to that of Pt at operating potentials of fuel cell cathodes [264]. Zhang *et al.* [194] prepared PdFe-nanoleaves with Pd-rich nanowires surrounded by Fe-rich sheets. The structure demonstrated three times increased specific activity and 2.7 times increased mass activity compared with a commercial Pt/C catalyst.

5.5. Single Fuel Cell Characterizations

Two kinds of fuel cells, the PEMFC feeding with H₂/O₂ and direct alcohol (ethanol or methanol) fuel cells, were studied by using above mentioned catalysts. In PEMFC applications, Tang *et al.* [195] proved

the performance of Pd/C was much less than that of the commercial Pt/C. Single cell with Pd/C as the cathode displayed a maximum power density of 508 mW cm^{-2} which was almost half of that of commercial Pt/C catalyst. This result was the same with the half cell test, that is, the performance of Pd/C catalyst was much inferior to that of the Pt/C catalyst for the ORR. Thanasilp *et al.* [256] studied the influence of Pt:Pd atomic ratios on a carbon supported upon its suitability as a cathode for a PEMFC. Although the different Pt:Pd atomic ratios had a significant effect on the performance in a H_2/O_2 fuel cell, the performance of the PdPt alloy was still much lower than that of Pt/C catalyst. Rosa *et al.* [274] directly sprayed Pd ink on carbon paper to form a novel oxygen diffusion electrode for the PEMFC, but the utilization efficiency of Pd was not satisfactory. With the help of nanotechnology, the performance of Pd catalyst with novel nano-structures as the PEMFC cathode was greatly improved. Li *et al.* [211] synthesized PdFe nanorods with tunable length which showed a better PEMFC performance than that of the commercial Pt/C due to their high intrinsic activity to ORR at reduced cell inner resistance and improved mass transport.

In direct alcohol fuel cells, Xu *et al.* [241] studied Au-modified Pd catalysts on carbon nanotubes which yielded a peak power density of 1.4 times higher than that with the mono-Pd cathode but was still less than Pt cathode. Pd alloys such as PdCoMo alloy [199] and PdCo alloy [199] showed comparable performance with that of commercial Pt/C, the PdNi alloy showed much higher performance than of Pd/C but still inferior to that of Pt/C catalyst [260]. It turns out that alloying Pd with other metals like Fe, Co and Ni is possible to improve the performance, reduce the cost and improve the stability of fuel cell.

6. Conclusions and Future Perspective

This article reviewed the latest advances in Pd-based catalysts for fuel cells. The review focused on Pd nanostructure, Pd catalysts for formic acid oxidation, alcohol oxidation and oxygen reduction reaction.

Different Pd morphologies were prepared. Due to the intrinsic advantages in crystallography and morphology, most of the Pd nanomaterials have high performance in fuel cell half cell characterization. Both the activity and stability of the catalysts could be improved, which would significantly reduce the usage of Pd in fuel cells. But the nano-structured Pd could not be vast applied in fuel cell, because of the limited yield and the difficulty in the MEA preparation. Future studies should be conducted to realize the mass production and find ways for efficient MEA preparing techniques.

As fuel cell catalysts for formic acid oxidation, methanol oxidation and oxygen reduction, Pd was loaded on carbon powders or other novel supports such as graphene and carbon nanotubes to achieve high electrochemical active surface area and improve the utilization efficiency of the Pd catalyst. The nature of the support materials also had great influence on the activity of Pd catalyst. Supported Pd nano-structures often had better performance than particles. Alloying with other metals could modify the electronic structure and induce tensile strain of the Pd clusters and finally influence their catalytic activities. There was great potential in the development of Pd alloy catalysts especially with non-noble metals to perform improved performance and stability and at the same time the reduced cost.

Considering the cost and comparable activity with Pt, the Pd-based catalysts are potential candidates as main catalysts for fuel cells to reduce the use of Pt and the cost for commercialization.

Acknowledgments

This work was supported by National Natural Science Foundation of China (21106190, 21476096, 51303217); Pearl River S&T Nova Program of Guangzhou (2013J2200040); Blue Ocean Talent Project of Nanhai, Foshan; 44th Scientific Research Foundation for the Returned Overseas Chinese Scholars, State Education Ministry; Key Laboratory of Functional Inorganic Material Chemistry (Heilongjiang University), Ministry of Education; the Fundamental Research Funds for the Central Universities.

Author Contributions

Hui Meng wrote the review and designed the structure. Fangyan Xie and Dongrong Zeng collected and classified the references.

Conflicts of Interest

The authors declare no conflict of interest.

References

1. Grove, W.R. XXIV. On voltaic series and the combination of gases by platinum. *Philos. Mag. Ser.* **1839**, *14*, 127–130.
2. Soszko, M.; Lukaszewski, M.; Mianowska, Z.; Czerwinski, A. Electrochemical characterization of the surface and methanol electrooxidation on Pt–Rh–Pd ternary alloys. *J. Power Sources* **2011**, *196*, 3513–3522.
3. Shao, M. Palladium-based electrocatalysts for hydrogen oxidation and oxygen reduction reactions. *J. Power Sources* **2011**, *196*, 2433–2444.
4. Palladium Chart—Last 5 years. Available online: <http://www.kitco.com/charts/popup/pd1825nyb.html> (accessed on 1 May 2015).
5. Bianchini, C.; Shen, P.K. Palladium-Based Electrocatalysts for Alcohol Oxidation in Half Cells and in Direct Alcohol Fuel Cells. *Chem. Rev.* **2009**, *109*, 4183–4206.
6. Antolini, E. Palladium in fuel cell catalysis. *Energy Environ. Sci.* **2009**, *2*, 915–931.
7. Mazumder, V.; Lee, Y.; Sun, S.H. Recent Development of Active Nanoparticle Catalysts for Fuel Cell Reactions. *Adv. Funct. Mater.* **2010**, *20*, 1224–1231.
8. Antolini, E.; Gonzalez, E.R. Alkaline direct alcohol fuel cells. *J. Power Sources* **2010**, *195*, 3431–3450.
9. Morozan, A.; Josselme, B.; Palacin, S. Low-platinum and platinum-free catalysts for the oxygen reduction reaction at fuel cell cathodes. *Energy Environ. Sci.* **2011**, *4*, 1238–1254.
10. Zhao, X.; Yin, M.; Ma, L.; Liang, L.; Liu, C.P.; Liao, J.H.; Lu, T.H.; Xing, W. Recent advances in catalysts for direct methanol fuel cells. *Energy Environ. Sci.* **2011**, *4*, 2736–2753.
11. Adams, B.D.; Chen, A.C. The role of palladium in a hydrogen economy. *Mater. Today* **2011**, *14*, 282–289.
12. Zhou, Z.Y.; Tian, N.; Li, J.T.; Broadwell, I.; Sun, S.G. Nanomaterials of high surface energy with exceptional properties in catalysis and energy storage. *Chem. Soc. Rev.* **2011**, *40*, 4167–4185.

13. Tian, N.; Zhou, Z.Y.; Yu, N.F.; Wang, L.Y.; Sun, S.G. Direct Electrodeposition of Tetrahedral Pd Nanocrystals with High-Index Facets and High Catalytic Activity for Ethanol Electrooxidation. *J. Am. Chem. Soc.* **2010**, *132*, 7580–7581.
14. Zhou, Z.Y.; Tian, N.; Huang, Z.Z.; Chen, D.J.; Sun, S.G. Nanoparticle catalysts with high energy surfaces and enhanced activity synthesized by electrochemical method. *Faraday Discuss.* **2008**, *140*, 81–92.
15. Shen, Q.M.; Min, Q.H.; Shi, J.J.; Jiang, L.P.; Zhang, J.R.; Hou, W.H.; Zhu, J.J. Morphology-Controlled Synthesis of Palladium Nanostructures by Sonoelectrochemical Method and Their Application in Direct Alcohol Oxidation. *J. Phys. Chem. C* **2009**, *113*, 1267–1273.
16. Ding, H.; Shi, X.Z.; Shen, C.M.; Hui, C.; Xu, Z.C.; Li, C.; Tian, Y.A.; Wang, D.K.; Gao, H.J. Synthesis of monodisperse palladium nanocubes and their catalytic activity for methanol electrooxidation. *Chin. Phys. B* **2010**, *19*, doi:10.1088/1674-1056/19/10/106104.
17. Yin, Z.; Zheng, H.J.; Ma, D.; Bao, X.H. Porous Palladium Nanoflowers that Have Enhanced Methanol Electro-Oxidation Activity. *J. Phys. Chem. C* **2009**, *113*, 1001–1005.
18. Meng, H.; Sun, S.; Masse, J.P.; Dodelet, J.P. Electrosynthesis of Pd Single-Crystal Nanothorns and Their Application in the Oxidation of Formic Acid. *Chem. Mater.* **2008**, *20*, 6998–7002.
19. Meng, H.; Wang, C.X.; Shen, P.K.; Wu, G. Palladium thorn clusters as catalysts for electrooxidation of formic acid. *Energy Environ. Sci.* **2011**, *4*, 1522–1526.
20. Tian, N.; Zhou, Z.Y.; Sun, S.G. Electrochemical preparation of Pd nanorods with high-index facets. *Chem. Commun.* **2009**, 1502–1504.
21. Patra, S.; Viswanath, B.; Barai, K.; Ravishankar, N.; Munichandraiah, N. High-Surface Step Density on Dendritic Pd Leads to Exceptional Catalytic Activity for Formic Acid Oxidation. *ACS Appl. Mater. Interfaces* **2010**, *2*, 2965–2969.
22. Zhang, J.; Cheng, Y.; Lu, S.F.; Jia, L.C.; Shen, P.K.; Jiang, S.P. Significant promotion effect of carbon nanotubes on the electrocatalytic activity of supported Pd NPs for ethanol oxidation reaction of fuel cells: The role of inner tubes. *Chem. Commun.* **2014**, *50*, 13732–13734.
23. Du, C.Y.; Chen, M.; Wang, W.G.; Yin, G.P. Nanoporous PdNi Alloy Nanowires As Highly Active Catalysts for the Electro-Oxidation of Formic Acid. *ACS Appl. Mater. Interfaces* **2011**, *3*, 105–109.
24. Lee, Y.W.; Lim, M.A.; Kang, S.W.; Park, I.; Han, S.W. Facile synthesis of noble metal nanotubes by using ZnO nanowires as sacrificial scaffolds and their electrocatalytic properties. *Chem. Commun.* **2011**, *47*, 6299–6301.
25. Wen, D.; Guo, S.J.; Dong, S.J.; Wang, E.K. Ultrathin Pd nanowire as a highly active electrode material for sensitive and selective detection of ascorbic acid. *Biosens. Bioelectron.* **2010**, *26*, 1056–1061.
26. Jena, B.K.; Sahu, S.C.; Satpati, B.; Sahu, R.K.; Behera, D.; Mohanty, S. A facile approach for morphosynthesis of Pd nanoelectrocatalysts. *Chem. Commun.* **2011**, *47*, 3796–3798.
27. Zhou, R.; Zhou, W.Q.; Zhang, H.M.; Du, Y.K.; Yang, P.; Wang, C.Y.; Xu, J.K. Facile template-free synthesis of pine needle-like Pd micro/nano-leaves and their associated electro-catalytic activities toward oxidation of formic acid. *Nanoscale Res. Lett.* **2011**, *6*, doi:10.1186/1556-276X-6-381.

28. Yu, J.S.; Fujita, T.; Inoue, A.; Sakurai, T.; Chen, M.W. Electrochemical synthesis of palladium nanostructures with controllable morphology. *Nanotechnology* **2010**, *21*, doi:10.1088/0957-4484/21/8/085601.
29. Fang, Y.X.; Guo, S.J.; Zhu, C.Z.; Dong, S.J.; Wang, E.K. Twenty Second Synthesis of Pd Nanourchins with High Electrochemical Activity through an Electrochemical Route. *Langmuir* **2010**, *26*, 17816–17820.
30. Li, L.Q.; E, Y.; Yuan, J.M.; Luo, X.Y.; Yang, Y.; Fan, L.Z. Electrosynthesis of Pd/Au hollow cone-like microstructures for electrocatalytic formic acid oxidation. *Electrochim. Acta* **2011**, *56*, 6237–6244.
31. Ye, L.; Wang, Y.; Chen, X.Y.; Yue, B.; Tsang, S.C.; He, H.Y. Three-dimensionally ordered mesoporous Pd networks templated by a silica super crystal and their application in formic acid electrooxidation. *Chem. Commun.* **2011**, *47*, 7389–7391.
32. Carrera-Cerritos, R.; Fuentes-Ramirez, R.; Cuevas-Muniz, F.M.; Ledesma-Garcia, J.; Arriaga, L.G. Performance and stability of Pd nanostructures in an alkaline direct ethanol fuel cell. *J. Power Sources* **2014**, *269*, 370–378.
33. Choi, S.I.; Shao, M.H.; Lu, N.; Ruditskiy, A.; Peng, H.C.; Park, J.; Guerrero, S.; Wang, J.G.; Kim, M.J.; Xia, Y.N. Synthesis and Characterization of Pd@Pt–Ni Core-Shell Octahedra with High Activity toward Oxygen Reduction. *ACS Nano* **2014**, *8*, 10363–10371.
34. Lim, Y.; Kim, S.K.; Lee, S.C.; Choi, J.; Nahm, K.S.; Yoo, S.J.; Kim, P. One-step synthesis of carbon-supported Pd@Pt/C core-shell nanoparticles as oxygen reduction electrocatalysts and their enhanced activity and stability. *Nanoscale* **2014**, *6*, 4038–4042.
35. Liu, Z.L.; Zhao, B.; Guo, C.L.; Sun, Y.J.; Shi, Y.; Yang, H.B.; Li, Z.A. Carbon nanotube/raspberry hollow Pd nanosphere hybrids for methanol, ethanol, and formic acid electro-oxidation in alkaline media. *J. Colloid Interface Sci.* **2010**, *351*, 233–238.
36. Bai, Z.Y.; Yang, L.; Li, L.; Lv, J.; Wang, K.; Zhang, J. A Facile Preparation of Hollow Palladium Nanosphere Catalysts for Direct Formic Acid Fuel Cell. *J. Phys. Chem. C* **2009**, *113*, 10568–10573.
37. Fang, P.P.; Duan, S.; Lin, X.D.; Anema, J.R.; Li, J.F.; Buriez, O.; Ding, Y.; Fan, F.R.; Wu, D.Y.; Ren, B.; *et al.* Tailoring Au-core Pd-shell Pt-cluster nanoparticles for enhanced electrocatalytic activity. *Chem. Sci.* **2011**, *2*, 531–539.
38. Ksar, F.; Ramos, L.; Keita, B.; Nadjo, L.; Beaunier, P.; Remita, H. Bimetallic Palladium-Gold Nanostructures: Application in Ethanol Oxidation. *Chem. Mater.* **2009**, *21*, 3677–3683.
39. Hsu, C.J.; Huang, C.W.; Hao, Y.W.; Liu, F.Q. Au/Pd core-shell nanoparticles with varied hollow Au cores for enhanced formic acid oxidation. *Nanoscale Res. Lett.* **2013**, *8*, doi:10.1186/1556-276X-8-113.
40. Kim, D.Y.; Kang, S.W.; Choi, K.W.; Choi, S.W.; Han, S.W.; Im, S.H.; Park, O.O. Au@Pd nanostructures with tunable morphologies and sizes and their enhanced electrocatalytic activity. *Crystengcomm* **2013**, *15*, 7113–7120.
41. Miao, F.J.; Tao, B.R.; Sun, L.; Liu, T.; You, J.C.; Wang, L.W.; Chu, P.K. Preparation and characterization of novel nickel-palladium electrodes supported by silicon microchannel plates for direct methanol fuel cells. *J. Power Sources* **2010**, *195*, 146–150.

42. Mikolajczuk, A.; Borodzinski, A.; Kedzierzawski, P.; Stobinski, L.; Mierzwa, B.; Dziura, R. Deactivation of carbon supported palladium catalyst in direct formic acid fuel cell. *Appl. Surface Sci.* **2011**, *257*, 8211–8214.
43. Haan, J.L.; Stafford, K.M.; Masel, R.I. Effects of the Addition of Antimony, Tin, and Lead to Palladium Catalyst Formulations for the Direct Formic Acid Fuel Cell. *J. Phys. Chem. C* **2010**, *114*, 11665–11672.
44. Xu, W.F.; Gao, Y.; Lu, T.H.; Tang, Y.W.; Wu, B. Kinetic Study of Formic Acid Oxidation on Highly Dispersed Carbon Supported Pd-TiO₂ Electrocatalyst. *Catal. Lett.* **2009**, *130*, 312–317.
45. Zhang, H.X.; Wang, C.; Wang, J.Y.; Zhai, J.J.; Cai, W.B. Carbon-Supported Pd-Pt Nanoalloy with Low Pt Content and Superior Catalysis for Formic Acid Electro-oxidation. *J. Phys. Chem. C* **2010**, *114*, 6446–6451.
46. Morales-Acosta, D.; Ledesma-Garcia, J.; Godinez, L.A.; Rodriguez, H.G.; Alvarez-Contreras, L.; Arriaga, L.G. Development of Pd and Pd-Co catalysts supported on multi-walled carbon nanotubes for formic acid oxidation. *J. Power Sources* **2010**, *195*, 461–465.
47. Du, C.Y.; Chen, M.; Wang, W.G.; Yin, G.P.; Shi, P.F. Electrodeposited PdNi₂ alloy with novelly enhanced catalytic activity for electrooxidation of formic acid. *Electrochem. Commun.* **2010**, *12*, 843–846.
48. Wu, Y.N.; Liao, S.J.; Su, Y.L.; Zeng, J.F.; Dang, D. Enhancement of anodic oxidation of formic acid on palladium decorated Pt/C catalyst. *J. Power Sources* **2010**, *195*, 6459–6462.
49. Zhou, Z.Y.; Kang, X.W.; Song, Y.; Chen, S.W. Butylphenyl-functionalized palladium nanoparticles as effective catalysts for the electrooxidation of formic acid. *Chem. Commun.* **2011**, *47*, 6075–6077.
50. Wang, X.M.; Wang, M.E.; Zhou, D.D.; Xia, Y.Y. Structural design and facile synthesis of a highly efficient catalyst for formic acid electrooxidation. *Phys. Chem. Chem. Phys.* **2011**, *13*, 13594–13597.
51. Ge, J.J.; Chen, X.M.; Liu, C.P.; Lu, T.H.; Liao, J.H.; Liang, L.A.; Xing, W. Promoting effect of vanadium ions on the anodic Pd/C catalyst for direct formic acid fuel cell application. *Electrochim. Acta* **2010**, *55*, 9132–9136.
52. Liang, Y.; Zhu, M.N.; Ma, J.; Tang, Y.W.; Chen, Y.; Lu, T.H. Highly dispersed carbon-supported Pd nanoparticles catalyst synthesized by novel precipitation-reduction method for formic acid electrooxidation. *Electrochim. Acta* **2011**, *56*, 4696–4702.
53. Zhang, Z.H.; Ge, J.J.; Ma, L.A.; Liao, J.H.; Lu, T.H.; Xing, W. Highly Active Carbon-supported PdSn Catalysts for Formic Acid Electrooxidation. *Fuel Cells* **2009**, *9*, 114–120.
54. Wang, X.M.; Wang, J.; Zou, Q.Q.; Xia, Y.Y. Pd nanoparticles supported on carbon-modified rutile TiO₂ as a highly efficient catalyst for formic acid electrooxidation. *Electrochim. Acta* **2011**, *56*, 1646–1651.
55. Cui, Z.M.; Kulesza, P.J.; Li, C.M.; Xing, W.; Jiang, S.P. Pd nanoparticles supported on HPMo-PDDA-MWCNT and their activity for formic acid oxidation reaction of fuel cells. *Int. J. Hydrogen Energy* **2011**, *36*, 8508–8517.
56. Pandey, R.K.; Lakshminarayanan, V. Electro-Oxidation of Formic Acid, Methanol, and Ethanol on Electrodeposited Pd-Polyaniline Nanofiber Films in Acidic and Alkaline Medium. *J. Phys. Chem. C* **2009**, *113*, 21596–21603.

57. Park, I.S.; Lee, K.S.; Yoo, S.J.; Cho, Y.H.; Sung, Y.E. Electrocatalytic properties of Pd clusters on Au nanoparticles in formic acid electro-oxidation. *Electrochim. Acta* **2010**, *55*, 4339–4345.
58. Zhao, H.; Yang, J.; Wang, L.; Tian, C.G.; Jiang, B.J.; Fu, H.G. Fabrication of a palladium nanoparticle/graphene nanosheet hybrid via sacrifice of a copper template and its application in catalytic oxidation of formic acid. *Chem. Commun.* **2011**, *47*, 2014–2016.
59. Yang, J.; Tian, C.G.; Wang, L.; Fu, H.G. An effective strategy for small-sized and highly-dispersed palladium nanoparticles supported on graphene with excellent performance for formic acid oxidation. *J. Mater. Chem.* **2011**, *21*, 3384–3390.
60. Wang, X.G.; Wang, W.M.; Qi, Z.; Zhao, C.C.; Ji, H.; Zhang, Z.H. High catalytic activity of ultrafine nanoporous palladium for electro-oxidation of methanol, ethanol, and formic acid. *Electrochem. Commun.* **2009**, *11*, 1896–1899.
61. Winjobi, O.; Zhang, Z.Y.; Liang, C.H.; Li, W.Z. Carbon nanotube supported platinum-palladium nanoparticles for formic acid oxidation. *Electrochim. Acta* **2010**, *55*, 4217–4221.
62. Tu, D.D.; Wu, B.; Wang, B.X.; Deng, C.; Gao, Y. A highly active carbon-supported PdSn catalyst for formic acid electrooxidation. *Appl. Catal. B* **2011**, *103*, 163–168.
63. Hu, C.G.; Bai, Z.Y.; Yang, L.; Lv, J.; Wang, K.; Guo, Y.M.; Cao, Y.X.; Zhou, J.G. Preparation of high performance Pd catalysts supported on untreated multi-walled carbon nanotubes for formic acid oxidation. *Electrochim. Acta* **2010**, *55*, 6036–6041.
64. Gao, Y.W.; Wang, G.; Wu, B.; Deng, C.; Gao, Y. Highly active carbon-supported PdNi catalyst for formic acid electrooxidation. *J. Appl. Electrochem.* **2011**, *41*, 1–6.
65. Wang, J.Y.; Kang, Y.Y.; Yang, H.; Cai, W.B. Boron-Doped Palladium Nanoparticles on Carbon Black as a Superior Catalyst for Formic Acid Electro-oxidation. *J. Phys. Chem. C* **2009**, *113*, 8366–8372.
66. Zhang, G.J.; Wang, Y.E.; Wang, X.; Chen, Y.; Zhou, Y.M.; Tang, Y.W.; Lu, L.D.; Bao, J.C.; Lu, T.H. Preparation of Pd-Au/C catalysts with different alloying degree and their electrocatalytic performance for formic acid oxidation. *Appl. Catal. B* **2011**, *102*, 614–619.
67. Bai, Z.Y.; Guo, Y.M.; Yang, L.; Li, L.; Li, W.J.; Xu, P.L.; Hu, C.G.; Wang, K. Highly dispersed Pd nanoparticles supported on 1,10-phenanthroline-functionalized multi-walled carbon nanotubes for electrooxidation of formic acid. *J. Power Sources* **2011**, *196*, 6232–6237.
68. Bong, S.; Uhm, S.; Kim, Y.R.; Lee, J.; Kim, H. Graphene Supported Pd Electrocatalysts for Formic Acid Oxidation. *Electrocatalysis* **2010**, *1*, 139–143.
69. Hu, G.Z.; Nitze, F.; Barzegar, H.R.; Sharifi, T.; Mikolajczuk, A.; Tai, C.W.; Borodzinski, A.; Wagberg, T. Palladium nanocrystals supported on helical carbon nanofibers for highly efficient electro-oxidation of formic acid, methanol and ethanol in alkaline electrolytes. *J. Power Sources* **2012**, *209*, 236–242.
70. Nitze, F.; Mazurkiewicz, M.; Malolepszy, A.; Mikolajczuk, A.; Kedzierzawski, P.; Tai, C.W.; Hu, G.Z.; Kurzydowski, K.J.; Stobinski, L.; Borodzinski, A.; *et al.* Synthesis of palladium nanoparticles decorated helical carbon nanofiber as highly active anodic catalyst for direct formic acid fuel cells. *Electrochim. Acta* **2012**, *63*, 323–328.
71. Feng, Y.Y.; Yin, Q.Y.; Lu, G.P.; Yang, H.F.; Zhu, X.; Kong, D.S.; You, J.M. Enhanced catalytic performance of Pd catalyst for formic acid electrooxidation in ionic liquid aqueous solution. *J. Power Sources* **2014**, *272*, 606–613.

72. Cheng, N.C.; Lv, H.F.; Wang, W.; Mu, S.C.; Pan, M.; Marken, F. An ambient aqueous synthesis for highly dispersed and active Pd/C catalyst for formic acid electro-oxidation. *J. Power Sources* **2010**, *195*, 7246–7249.
73. Suo, Y.; Hsing, I.M. Size-controlled synthesis and impedance-based mechanistic understanding of Pd/C nanoparticles for formic acid oxidation. *Electrochim. Acta* **2009**, *55*, 210–217.
74. Lee, J.Y.; Kwak, D.H.; Lee, Y.W.; Lee, S.; Park, K.W. Synthesis of cubic PtPd alloy nanoparticles as anode electrocatalysts for methanol and formic acid oxidation reactions. *Phys. Chem. Chem. Phys.* **2015**, *17*, 8642–8648.
75. Baranova, E.A.; Miles, N.; Mercier, P.H.J.; le Page, Y.; Patarachao, B. Formic acid electro-oxidation on carbon supported Pd_xPt_{1-x} (0 ≤ x ≤ 1) nanoparticles synthesized via modified polyol method. *Electrochim. Acta* **2010**, *55*, 8182–8188.
76. Matin, M.A.; Jang, J.H.; Lee, E.; Kwon, Y.U. Sonochemical synthesis of Pt-doped Pd nanoparticles with enhanced electrocatalytic activity for formic acid oxidation reaction. *J. Appl. Electrochem.* **2012**, *42*, 827–832.
77. Liu, Z.L.; Zhang, X.H. Carbon-supported PdSn nanoparticles as catalysts for formic acid oxidation. *Electrochem. Commun.* **2009**, *11*, 1667–1670.
78. Celorrio, V.; de Oca, M.G.M.; Plana, D.; Moliner, R.; Lazaro, M.J.; Fermin, D.J. Effect of Carbon Supports on Electrocatalytic Reactivity of Au-Pd Core-Shell Nanoparticles. *J. Phys. Chem. C* **2012**, *116*, 6275–6282.
79. Celorrio, V.; de Oca, M.G.M.; Plana, D.; Moliner, R.; Fermin, D.J.; Lazaro, M.J. Electrochemical performance of Pd and Au-Pd core-shell nanoparticles on surface tailored carbon black as catalyst support. *Int. J. Hydrogen Energy* **2012**, *37*, 7152–7160.
80. Wang, H.; Ge, X.B. Facile Fabrication of Porous Pd-Au Bimetallic Nanostructures for Electrocatalysis. *Electroanalysis* **2012**, *24*, 911–916.
81. Shi, R.R.; Wang, J.S.; Cheng, N.C.; Sun, X.L.; Zhang, L.; Zhang, J.J.; Wang, L.C. Electrocatalytic activity and stability of carbon nanotubes-supported Pt-on-Au, Pd-on-Au, Pt-on-Pd-on-Au, Pt-on-Pd, and Pd-on-Pt catalysts for methanol oxidation reaction. *Electrochim. Acta* **2014**, *148*, 1–7.
82. Li, G.Q.; Feng, L.G.; Chang, J.F.; Wickman, B.; Gronbeck, H.; Liu, C.P.; Xing, W. Activity of Platinum/Carbon and Palladium/Carbon Catalysts Promoted by Ni₂P in Direct Ethanol Fuel Cells. *Chemsuschem* **2014**, *7*, 3374–3381.
83. Liu, H.Q.; Koenigsmann, C.; Adzic, R.R.; Wong, S.S. Probing Ultrathin One-Dimensional Pd–Ni Nanostructures As Oxygen Reduction Reaction Catalysts. *ACS Catal.* **2014**, *4*, 2544–2555.
84. Yu, X.W.; Pickup, P.G. Novel Pd-Pb/C bimetallic catalysts for direct formic acid fuel cells. *J. Power Sources* **2009**, *192*, 279–284.
85. Feng, L.G.; Yang, J.; Hu, Y.; Zhu, J.B.; Liu, C.P.; Xing, W. Electrocatalytic properties of PdCeO_x/C anodic catalyst for formic acid electrooxidation. *Int. J. Hydrogen Energy* **2012**, *37*, 4812–4818.
86. Liu, Z.L.; Zhang, X.H.; Tay, S.W. Nanostructured PdRu/C catalysts for formic acid oxidation. *J. Solid State Electrochem.* **2012**, *16*, 545–550.
87. Arikan, T.; Kannan, A.M.; Kadirgan, F. Binary Pt–Pd and ternary Pt–Pd–Ru nanoelectrocatalysts for direct methanol fuel cells. *Int. J. Hydrogen Energy* **2013**, *38*, 2900–2907.

88. Awasthi, R.; Singh, R.N. Graphene-supported Pd–Ru nanoparticles with superior methanol electrooxidation activity. *Carbon* **2013**, *51*, 282–289.
89. Qin, Y.H.; Jia, Y.B.; Jiang, Y.; Niu, D.F.; Zhang, X.S.; Zhou, X.G.; Niu, L.; Yuan, W.K. Controllable synthesis of carbon nanofiber supported Pd catalyst for formic acid electrooxidation. *Int. J. Hydrogen Energy* **2012**, *37*, 7373–7377.
90. Li, Y.H.; Xu, Q.Z.; Li, Q.Y.; Wang, H.Q.; Huang, Y.G.; Xu, C.W. Pd deposited on MWCNTs modified carbon fiber paper as high-efficient electrocatalyst for ethanol electrooxidation. *Electrochim. Acta* **2014**, *147*, 151–156.
91. Chakraborty, S.; Raj, C.R. Electrocatalytic performance of carbon nanotube-supported palladium particles in the oxidation of formic acid and the reduction of oxygen. *Carbon* **2010**, *48*, 3242–3249.
92. Liu, J.; Liu, R.; Yuan, C.L.; Wei, X.P.; Yin, J.L.; Wang, G.L.; Cao, D.X. Pd-Co/MWCNTs Catalyst for Electrooxidation of Hydrazine in Alkaline Solution. *Fuel Cells* **2013**, *13*, 903–909.
93. Selvaraj, V.; Grace, A.N.; Alagar, M. Electrocatalytic oxidation of formic acid and formaldehyde on nanoparticle decorated single walled carbon nanotubes. *J. Colloid Interface Sci.* **2009**, *333*, 254–262.
94. Limpattayanate, S.; Hunsom, M. Electrocatalytic activity of Pt-Pd electrocatalysts for the oxygen reduction reaction in proton exchange membrane fuel cells: Effect of supports. *Renew. Energy* **2014**, *63*, 205–211.
95. Chen, C.H.; Liou, W.J.; Lin, H.M.; Wu, S.H.; Mikolajczuk, A.; Stobinski, L.; Borodzinski, A.; Kedzierzawski, P.; Kurzydowski, K. Carbon nanotube-supported bimetallic palladium-gold electrocatalysts for electro-oxidation of formic acid. *Phys. Status Solidi Appl. Mater. Sci.* **2010**, *207*, 1160–1165.
96. Chen, C.H.; Liou, W.J.; Lin, H.M.; Wu, S.H.; Borodzinski, A.; Stobinski, L.; Kedzierzawski, P. Palladium and Palladium Gold Catalysts Supported on MWCNTs for Electrooxidation of Formic Acid. *Fuel Cells* **2010**, *10*, 227–233.
97. Mikolajczuk, A.; Borodzinski, A.; Stobinski, L.; Kedzierzawski, P.; Lesiak, B.; Laszlo, K.; Jozsef, T.; Lin, H.M. Study of Pd-Au/MWCNTs formic acid electrooxidation catalysts. *Phys. Status Solidi B* **2010**, *247*, 2717–2721.
98. Qin, Y.H.; Jiang, Y.; Niu, D.F.; Zhang, X.S.; Zhou, X.G.; Niu, L.; Yuan, W.K. Carbon nanofiber supported bimetallic PdAu nanoparticles for formic acid electrooxidation. *J. Power Sources* **2012**, *215*, 130–134.
99. Wang, X.G.; Tang, B.; Huang, X.B.; Ma, Y.; Zhang, Z.H. High activity of novel nanoporous Pd-Au catalyst for methanol electro-oxidation in alkaline media. *J. Alloys Compd.* **2013**, *565*, 120–126.
100. Takenaka, S.; Tsukamoto, T.; Matsune, H.; Kishida, M. Carbon nanotube-supported Pd–Co catalysts covered with silica layers as active and stable cathode catalysts for polymer electrolyte fuel cells. *Catal. Sci. Technol.* **2013**, *3*, 2723–2731.
101. Yang, S.D.; Shen, C.M.; Lu, X.J.; Tong, H.; Zhu, J.J.; Zhang, X.G.; Gao, H.J. Preparation and electrochemistry of graphene nanosheets-multiwalled carbon nanotubes hybrid nanomaterials as Pd electrocatalyst support for formic acid oxidation. *Electrochim. Acta* **2012**, *62*, 242–249.

102. Qu, K.G.; Wu, L.; Ren, J.S.; Qu, X.G. Natural DNA-Modified Graphene/Pd Nanoparticles as Highly Active Catalyst for Formic Acid Electro-Oxidation and for the Suzuki Reaction. *ACS Appl. Mater. Interfaces* **2012**, *4*, 5001–5009.
103. Li, R.; Hao, H.; Huang, T.; Yu, A.S. Electrodeposited Pd–MoO_x catalysts with enhanced catalytic activity for formic acid electrooxidation. *Electrochim. Acta* **2012**, *76*, 292–299.
104. Lu, H.T.; Fan, Y.; Huang, P.; Xu, D.L. SnO₂ nanospheres supported Pd catalyst with enhanced performance for formic acid oxidation. *J. Power Sources* **2012**, *215*, 48–52.
105. Kim, I.T.; Choi, M.; Lee, H.K.; Shim, J. Characterization of methanol-tolerant Pd–WO₃ and Pd–SnO₂ electrocatalysts for the oxygen reduction reaction in direct methanol fuel cells. *J. Ind. Eng. Chem.* **2013**, *19*, 813–818.
106. Maheswari, S.; Sridhar, P.; Pitchumani, S. Pd–TiO₂/C as a methanol tolerant catalyst for oxygen reduction reaction in alkaline medium. *Electrochem. Commun.* **2013**, *26*, 97–100.
107. Matos, J.; Borodzinski, A.; Zychora, A.M.; Kedzierzawski, P.; Mierzwa, B.; Juchniewicz, K.; Mazurkiewicz, M.; Hernandez-Garrido, J.C. Direct formic acid fuel cells on Pd catalysts supported on hybrid TiO₂–C materials. *Appl. Catal. B* **2015**, *163*, 167–178.
108. Wang, X.M.; Xia, Y.Y. The influence of the crystal structure of TiO₂ support material on Pd catalysts for formic acid electrooxidation. *Electrochim. Acta* **2010**, *55*, 851–856.
109. Liao, M.Y.; Hu, Q.; Zheng, J.B.; Li, Y.H.; Zhou, H.; Zhong, C.J.; Chen, B.H. Pd decorated Fe/C nanocatalyst for formic acid electrooxidation. *Electrochim. Acta* **2013**, *111*, 504–509.
110. Bai, Z.Y.; Yang, L.; Guo, Y.M.; Zheng, Z.; Hu, C.G.; Xu, P.L. High-efficiency palladium catalysts supported on ppy-modified C-60 for formic acid oxidation. *Chem. Commun.* **2011**, *47*, 1752–1754.
111. Ding, K.Q.; Jia, H.T.; Wei, S.Y.; Guo, Z.H. Electrocatalysis of Sandwich-Structured Pd/Polypyrrole/Pd Composites toward Formic Acid Oxidation. *Ind. Eng. Chem. Res.* **2011**, *50*, 7077–7082.
112. Zhao, X.; Zhu, J.B.; Liang, L.; Liu, C.P.; Liao, J.H.; Xing, W. Enhanced electroactivity of Pd nanocrystals supported on H₃PMo₁₂O₄₀/carbon for formic acid electrooxidation. *J. Power Sources* **2012**, *210*, 392–396.
113. Qin, Y.H.; Yue, J.; Yang, H.H.; Zhang, X.S.; Zhou, X.G.; Niu, L.; Yuan, W.K. Synthesis of highly dispersed and active palladium/carbon nanofiber catalyst for formic acid electrooxidation. *J. Power Sources* **2011**, *196*, 4609–4612.
114. Cheng, N.C.; Webster, R.A.; Pan, M.; Mu, S.C.; Rassaei, L.; Tsang, S.C.; Marken, F. One-step growth of 3–5 nm diameter palladium electrocatalyst in a carbon nanoparticle-chitosan host and characterization for formic acid oxidation. *Electrochim. Acta* **2010**, *55*, 6601–6610.
115. Zhang, B.A.; Ye, D.D.; Li, J.; Zhu, X.; Liao, Q. Electrodeposition of Pd catalyst layer on graphite rod electrodes for direct formic acid oxidation. *J. Power Sources* **2012**, *214*, 277–284.
116. Liu, S.L.; Han, M.; Shi, Y.; Zhang, C.Z.; Chen, Y.; Bao, J.C.; Dai, Z.H. Gram-Scale Synthesis of Multipod Pd Nanocrystals by a Simple Solid-Liquid Phase Reaction and Their Remarkable Electrocatalytic Properties. *Eur. J. Inorg. Chem.* **2012**, *2012*, 3740–3746.
117. Xu, C.X.; Liu, Y.Q.; Wang, J.P.; Geng, H.R.; Qiu, H.J. Nanoporous PdCu alloy for formic acid electro-oxidation. *J. Power Sources* **2012**, *199*, 124–131.

118. Meng, H.; Xie, F.Y.; Chen, J.; Shen, P.K. Electrodeposited palladium nanostructure as novel anode for direct formic acid fuel cell. *J. Mater. Chem.* **2011**, *21*, 11352–11358.
119. Cheng, T.T.; Gyenge, E.L. Novel catalyst-support interaction for direct formic acid fuel cell anodes: Pd electrodeposition on surface-modified graphite felt. *J. Appl. Electrochem.* **2009**, *39*, 1925–1938.
120. Mikolajczuk, A.; Borodzinski, A.; Stobinski, L.; Kedzierzawski, P.; Lesiak, B.; Kover, L.; Toth, J.; Lin, H.M. Physicochemical characterization of the Pd/MWCNTs catalysts for fuel cell applications. *Phys. Status Solidi B* **2010**, *247*, 3063–3067.
121. Morales-Acosta, D.; Rodriguez, H.; Godinez, L.A.; Arriaga, L.G. Performance increase of microfluidic formic acid fuel cell using Pd/MWCNTs as catalyst. *J. Power Sources* **2010**, *195*, 1862–1865.
122. Yu, X.W.; Pickup, P.G. Screening of PdM and PtM catalysts in a multi-anode direct formic acid fuel cell. *J. Appl. Electrochem.* **2011**, *41*, 589–597.
123. Yan, Z.X.; Xie, J.M.; Shen, P.K.; Zhang, M.M.; Zhang, Y.; Chen, M. Pd supported on 2–4 nm MoC particles with reduced particle size, synergistic effect and high stability for ethanol oxidation. *Electrochim. Acta* **2013**, *108*, 644–650.
124. Jung, W.S.; Han, J.; Yoon, S.P.; Nam, S.W.; Lim, T.H.; Hong, S.A. Performance degradation of direct formic acid fuel cell incorporating a Pd anode catalyst. *J. Power Sources* **2011**, *196*, 4573–4578.
125. Ren, M.J.; Kang, Y.Y.; He, W.; Zou, Z.Q.; Xue, X.Z.; Akins, D.L.; Yang, H.; Feng, S.L. Origin of performance degradation of palladium-based direct formic acid fuel cells. *Appl. Catal. B* **2011**, *104*, 49–53.
126. Zhou, Y.; Liu, J.G.; Ye, J.L.; Zou, Z.G.; Ye, J.H.; Gu, J.; Yu, T.; Yang, A.D. Poisoning and regeneration of Pd catalyst in direct formic acid fuel cell. *Electrochim. Acta* **2010**, *55*, 5024–5027.
127. Yu, X.W.; Pickup, P.G. Deactivation/reactivation of a Pd/C catalyst in a direct formic acid fuel cell (DFAFC): Use of array membrane electrode assemblies. *J. Power Sources* **2009**, *187*, 493–499.
128. Chen, Y.X.; Lavacchi, A.; Chen, S.P.; di Benedetto, F.; Bevilacqua, M.; Bianchini, C.; Fornasiero, P.; Innocenti, M.; Marelli, M.; Oberhauser, W.; *et al.* Electrochemical Milling and Faceting: Size Reduction and Catalytic Activation of Palladium Nanoparticles. *Angew. Chem. Int. Ed.* **2012**, *51*, 8500–8504.
129. Wu, Q.M.; Rao, Z.X.; Yuan, L.Z.; Jiang, L.H.; Sun, G.Q.; Ruan, J.M.; Zhou, Z.C.; Sang, S.B. Carbon supported PdO with improved activity and stability for oxygen reduction reaction in alkaline solution. *Electrochim. Acta* **2014**, *150*, 157–166.
130. Yan, Z.X.; Hu, Z.F.; Chen, C.; Meng, H.; Shen, P.K.; Ji, H.B.; Meng, Y.Z. Hollow carbon hemispheres supported palladium electrocatalyst at improved performance for alcohol oxidation. *J. Power Sources* **2010**, *195*, 7146–7151.
131. Maiyalagan, T.; Scott, K. Performance of carbon nanofiber supported Pd–Ni catalysts for electro-oxidation of ethanol in alkaline medium. *J. Power Sources* **2010**, *195*, 5246–5251.
132. Xu, J.B.; Zhao, T.S.; Shen, S.Y.; Li, Y.S. Stabilization of the palladium electrocatalyst with alloyed gold for ethanol oxidation. *Int. J. Hydrogen Energy* **2010**, *35*, 6490–6500.

133. Cheng, F.L.; Dai, X.C.; Wang, H.; Jiang, S.P.; Zhang, M.; Xu, C.W. Synergistic effect of Pd–Au bimetallic surfaces in Au-covered Pd nanowires studied for ethanol oxidation. *Electrochim. Acta* **2010**, *55*, 2295–2298.
134. Gao, H.L.; Liao, S.J.; Liang, Z.X.; Liang, H.G.; Luo, F. Anodic oxidation of ethanol on core-shell structured Ru@PtPd/C catalyst in alkaline media. *J. Power Sources* **2011**, *196*, 6138–6143.
135. Bambagioni, V.; Bianchini, C.; Filippi, J.; Oberhauserl, W.; Marchionni, A.; Vizza, F.; Psaro, R.; Sordelli, L.; Foresti, M.L.; Innocenti, M. Ethanol Oxidation on Electrocatalysts Obtained by Spontaneous Deposition of Palladium onto Nickel-Zinc Materials. *Chemsuschem* **2009**, *2*, 99–112.
136. Chen, X.M.; Lin, Z.J.; Jia, T.T.; Cai, Z.M.; Huang, X.L.; Jiang, Y.Q.; Chen, X.; Chen, G.N. A facile synthesis of palladium nanoparticles supported on functional carbon nanotubes and its novel catalysis for ethanol electrooxidation. *Anal. Chim. Acta* **2009**, *650*, 54–58.
137. Fu, S.F.; Zhu, C.Z.; Du, D.; Lin, Y.H. Facile One-Step Synthesis of Three-Dimensional Pd–Ag Bimetallic Alloy Networks and Their Electrocatalytic Activity toward Ethanol Oxidation, *ACS Appl. Mater. Interfaces* **2015**, *7*, 13842–13848.
138. Lv, J.J.; Wisitruangsakul, N.; Feng, J.J.; Luo, J.; Fang, K.M.; Wang, A.J. Biomolecule-assisted synthesis of porous PtPd alloyed nanoflowers supported on reduced graphene oxide with highly electrocatalytic performance for ethanol oxidation and oxygen reduction, *Electrochim. Acta* **2015**, *160*, 100–107.
139. Wang, A.L.; He, X.J.; Lu, X.F.; Xu, H.; Tong, Y.X.; Li, G.R. Palladium-Cobalt Nanotube Arrays Supported on Carbon Fiber Cloth as High-Performance Flexible Electrocatalysts for Ethanol Oxidation. *Angew. Chem. Int. Ed.* **2015**, *54*, 3669–3673.
140. Ma, J.W.; Wang, J.; Zhang, G.H.; Fan, X.B.; Zhang, G.L.; Zhang, F.B.; Li, Y. Deoxyribonucleic acid-directed growth of well dispersed nickel-palladium-platinum nanoclusters on graphene as an efficient catalyst for ethanol electrooxidation. *J. Power Sources* **2015**, *278*, 43–49.
141. Peng, C.; Hu, Y.L.; Liu, M.R.; Zheng, Y.X., Hollow raspberry-like PdAg alloy nanospheres: High electrocatalytic activity for ethanol oxidation in alkaline media. *J. Power Sources* **2015**, *278*, 69–75.
142. Singh, R.N.; Awasthi, R. Graphene support for enhanced electrocatalytic activity of Pd for alcohol oxidation. *Catal. Sci. Technol.* **2011**, *1*, 778–783.
143. Su, L.; Jia, W.Z.; Schempf, A.; Ding, Y.; Lei, Y. Free-Standing Palladium/Polyamide 6 Nanofibers for Electrooxidation of Alcohols in Alkaline Medium. *J. Phys. Chem. C* **2009**, *113*, 16174–16180.
144. Wang, Y.L.; Zhao, Y.Q.; Xu, C.L.; Zhao, D.D.; Xu, M.W.; Su, Z.X.; Li, H.L. Improved performance of Pd electrocatalyst supported on three-dimensional nickel foam for direct ethanol fuel cells. *J. Power Sources* **2010**, *195*, 6496–6499.
145. Thotiyl, M.M.O.; Kumar, T.R.; Sampath, S. Pd Supported on Titanium Nitride for Efficient Ethanol Oxidation. *J. Phys. Chem. C* **2010**, *114*, 17934–17941.
146. Mahendiran, C.; Maiyalagan, T.; Scott, K.; Gedanken, A. Synthesis of a carbon-coated NiO/MgO core/shell nanocomposite as a Pd electro-catalyst support for ethanol oxidation. *Mater. Chem. Phys.* **2011**, *128*, 341–347.
147. Yi, Q.F.; Niu, F.J.; Sun, L.Z. Fabrication of novel porous Pd particles and their electroactivity towards ethanol oxidation in alkaline media. *Fuel* **2011**, *90*, 2617–2623.

148. Wang, X.G.; Wang, W.M.; Qi, Z.; Zhao, C.C.; Ji, H.; Zhang, Z.H. Fabrication, microstructure and electrocatalytic property of novel nanoporous palladium composites. *J. Alloys Compd.* **2010**, *508*, 463–470.
149. Liu, R.; Liu, J.F.; Jiang, G.B. Use of Triton X-114 as a weak capping agent for one-pot aqueous phase synthesis of ultrathin noble metal nanowires and a primary study of their electrocatalytic activity. *Chem. Commun.* **2010**, *46*, 7010–7012.
150. Ksar, F.; Surendran, G.; Ramos, L.; Keita, B.; Nadjo, L.; Prouzet, E.; Beaunier, P.; Hagege, A.; Audonnet, F.; Remita, H. Palladium Nanowires Synthesized in Hexagonal Mesophases: Application in Ethanol Electrooxidation. *Chem. Mater.* **2009**, *21*, 1612–1617.
151. Cherevko, S.; Xing, X.L.; Chung, C.H. Pt and Pd decorated Au nanowires: Extremely high activity of ethanol oxidation in alkaline media. *Electrochim. Acta* **2011**, *56*, 5771–5775.
152. Lin, S.C.; Chen, J.Y.; Hsieh, Y.F.; Wu, P.W. A facile route to prepare PdPt alloys for ethanol electro-oxidation in alkaline electrolyte. *Mater. Lett.* **2011**, *65*, 215–218.
153. Modibedi, R.M.; Masombuka, T.; Mathe, M.K. Carbon supported Pd-Sn and Pd-Ru-Sn nanocatalysts for ethanol electro-oxidation in alkaline medium. *Int. J. Hydrogen Energy* **2011**, *36*, 4664–4672.
154. Jou, L.H.; Chang, J.K.; Whang, T.J.; Sun, I.W. Electrodeposition of Palladium-Tin Alloys from 1-Ethyl-3-methylimidazolium Chloride-Tetrafluoroborate Ionic Liquid for Ethanol Electro-Oxidation. *J. Electrochem. Soc.* **2010**, *157*, D443–D449.
155. Shen, S.Y.; Zhao, T.S.; Xu, J.B. Carbon-supported bimetallic PdIr catalysts for ethanol oxidation in alkaline media. *Electrochim. Acta* **2010**, *55*, 9179–9184.
156. Qiu, C.C.; Shang, R.; Xie, Y.F.; Bu, Y.R.; Li, C.Y.; Ma, H.Y. Electrocatalytic activity of bimetallic Pd-Ni thin films towards the oxidation of methanol and ethanol. *Mater. Chem. Phys.* **2010**, *120*, 323–330.
157. Qi, Z.; Geng, H.R.; Wang, X.G.; Zhao, C.C.; Ji, H.; Zhang, C.; Xu, J.L.; Zhang, Z.H. Novel nanocrystalline PdNi alloy catalyst for methanol and ethanol electro-oxidation in alkaline media. *J. Power Sources* **2011**, *196*, 5823–5828.
158. Nguyen, S.T.; Law, H.M.; Nguyen, H.T.; Kristian, N.; Wang, S.Y.; Chan, S.H.; Wang, X. Enhancement effect of Ag for Pd/C towards the ethanol electro-oxidation in alkaline media. *Appl. Catal. B* **2009**, *91*, 507–515.
159. Oliveira, M.C.; Rego, R.; Fernandes, L.S.; Tavares, P.B. Evaluation of the catalytic activity of Pd-Ag alloys on ethanol oxidation and oxygen reduction reactions in alkaline medium. *J. Power Sources* **2011**, *196*, 6092–6098.
160. Wang, Y.; Nguyen, T.S.; Liu, X.W.; Wang, X. Novel palladium-lead (Pd-Pb/C) bimetallic catalysts for electrooxidation of ethanol in alkaline media. *J. Power Sources* **2010**, *195*, 2619–2622.
161. He, Q.G.; Chen, W.; Mukerjee, S.; Chen, S.W.; Laufek, F. Carbon-supported PdM (M = Au and Sn) nanocatalysts for the electrooxidation of ethanol in high pH media. *J. Power Sources* **2009**, *187*, 298–304.
162. Zhu, L.D.; Zhao, T.S.; Xu, J.B.; Liang, Z.X. Preparation and characterization of carbon-supported sub-monolayer palladium decorated gold nanoparticles for the electro-oxidation of ethanol in alkaline media. *J. Power Sources* **2009**, *187*, 80–84.

163. Hu, Z.F.; Yan, Z.X.; Shen, P.K.; Zhong, C.J. Nano-architectures of ordered hollow carbon spheres filled with carbon webs by template-free controllable synthesis. *Nanotechnology* **2012**, *23*, 48–53.
164. Yan, Z.X.; Meng, H.; Shen, P.K.; Meng, Y.Z.; Ji, H.B. Effect of the templates on the synthesis of hollow carbon materials as electrocatalyst supports for direct alcohol fuel cells. *Int. J. Hydrogen Energy* **2012**, *37*, 4728–4736.
165. Yan, Z.X.; Meng, H.; Shi, L.; Li, Z.H.; Shen, P.K. Synthesis of mesoporous hollow carbon hemispheres as highly efficient Pd electrocatalyst support for ethanol oxidation. *Electrochem. Commun.* **2010**, *12*, 689–692.
166. Cerritos, R.C.; Guerra-Balcazar, M.; Ramirez, R.F.; Ledesma-Garcia, J.; Arriaga, L.G. Morphological Effect of Pd Catalyst on Ethanol Electro-Oxidation Reaction. *Materials* **2012**, *5*, 1686–1697.
167. Ding, K.Q.; Yang, G.K. HCl-assisted pyrolysis of PdCl₂ to immobilize palladium nanoparticles on multi-walled carbon nanotubes. *Mater. Chem. Phys.* **2010**, *123*, 498–501.
168. Ding, K.Q.; Yang, G.K. Using RTILs of EMIBF₄ as “water” to prepare palladium nanoparticles onto MWCNTs by pyrolysis of PdCl₂. *Electrochim. Acta* **2010**, *55*, 2319–2324.
169. Chu, D.B.; Wang, J.; Wang, S.X.; Zha, L.W.; He, J.G.; Hou, Y.Y.; Yan, Y.X.; Lin, H.S.; Tian, Z.W. High activity of Pd–In₂O₃/CNTs electrocatalyst for electro-oxidation of ethanol. *Catal. Commun.* **2009**, *10*, 955–958.
170. Qin, Y.H.; Yang, H.H.; Zhang, X.S.; Li, P.; Ma, C.A. Effect of carbon nanofibers microstructure on electrocatalytic activities of Pd electrocatalysts for ethanol oxidation in alkaline medium. *Int. J. Hydrogen Energy* **2010**, *35*, 7667–7674.
171. Qin, Y.H.; Li, H.C.; Yang, H.H.; Zhang, X.S.; Zhou, X.G.; Niu, L.; Yuan, W.K. Effect of electrode fabrication methods on the electrode performance for ethanol oxidation. *J. Power Sources* **2011**, *196*, 159–163.
172. Qin, Y.H.; Yang, H.H.; Zhang, X.S.; Li, P.; Zhou, X.G.; Niu, L.; Yuan, W.K. Electrophoretic deposition of network-like carbon nanofibers as a palladium catalyst support for ethanol oxidation in alkaline media. *Carbon* **2010**, *48*, 3323–3329.
173. Wen, Z.L.; Yang, S.D.; Liang, Y.Y.; He, W.; Tong, H.; Hao, L.A.; Zhang, X.G.; Song, Q.J. The improved electrocatalytic activity of palladium/graphene nanosheets towards ethanol oxidation by tin oxide. *Electrochim. Acta* **2010**, *56*, 139–144.
174. Chen, X.M.; Wu, G.H.; Chen, J.M.; Chen, X.; Xie, Z.X.; Wang, X.R. Synthesis of “Clean” and Well-Dispersive Pd Nanoparticles with Excellent Electrocatalytic Property on Graphene Oxide. *J. Am. Chem. Soc.* **2011**, *133*, 3693–3695.
175. El-Shafei, A.A.; Elhafeez, A.M.A.; Mostafa, H.A. Ethanol oxidation at metal-zeolite-modified electrodes in alkaline medium. Part 2: Palladium-zeolite-modified graphite electrode. *J. Solid State Electrochem.* **2010**, *14*, 185–190.
176. Hasan, M.; Newcomb, S.B.; Rohan, J.F.; Razeeb, K.M. Ni nanowire supported 3D flower-like Pd nanostructures as an efficient electrocatalyst for electrooxidation of ethanol in alkaline media. *J. Power Sources* **2012**, *218*, 148–156.
177. Wang, W.J.; Zhang, J.; Yang, S.C.; Ding, B.J.; Song, X.P. Au@Pd Core-Shell Nanobricks with Concave Structures and Their Catalysis of Ethanol Oxidation. *Chemsuschem* **2013**, *6*, 1945–1951.

178. Li, S.J.; Cheng, D.J.; Qiu, X.G.; Cao, D.P. Synthesis of Cu@Pd core-shell nanowires with enhanced activity and stability for formic acid oxidation. *Electrochim. Acta* **2014**, *143*, 44–48.
179. Li, C.L.; Su, Y.; Lv, X.Y.; Shi, H.J.; Yang, X.G.; Wang, Y.J. Enhanced ethanol electrooxidation of hollow Pd nanospheres prepared by galvanic exchange reactions. *Mater. Lett.* **2012**, *69*, 92–95.
180. Wu, H.X.; Li, H.J.; Zhai, Y.J.; Xu, X.L.; Jin, Y.D. Facile Synthesis of Free-Standing Pd-Based Nanomembranes with Enhanced Catalytic Performance for Methanol/Ethanol Oxidation. *Adv. Mater.* **2012**, *24*, 1594–1597.
181. Ozturk, Z.; Sen, F.; Sen, S.; Gokagac, G. The preparation and characterization of nano-sized Pt-Pd/C catalysts and comparison of their superior catalytic activities for methanol and ethanol oxidation. *J. Mater. Sci.* **2012**, *47*, 8134–8144.
182. Shen, S.Y.; Zhao, T.S.; Xu, J.B.; Li, Y.S. Synthesis of PdNi catalysts for the oxidation of ethanol in alkaline direct ethanol fuel cells. *J. Power Sources* **2010**, *195*, 1001–1006.
183. Zhu, C.Z.; Guo, S.J.; Dong, S.J. PdM (M = Pt, Au) Bimetallic Alloy Nanowires with Enhanced Electrocatalytic Activity for Electro-oxidation of Small Molecules. *Adv. Mater.* **2012**, *24*, 2326–2331.
184. Seweryn, J.; Lewera, A. Electrooxidation of ethanol on carbon-supported Pt–Pd nanoparticles. *J. Power Sources* **2012**, *205*, 264–271.
185. Lv, J.J.; Zheng, J.N.; Zhang, H.B.; Lin, M.; Wang, A.J.; Chen, J.R.; Feng, J.J. Simple synthesis of platinum-palladium nanoflowers on reduced graphene oxide and their enhanced catalytic activity for oxygen reduction reaction. *J. Power Sources* **2014**, *269*, 136–143.
186. Ding, L.X.; Wang, A.L.; Ou, Y.N.; Li, Q.; Guo, R.; Zhao, W.X.; Tong, Y.X.; Li, G.R. Hierarchical Pd–Sn Alloy Nanosheet Dendrites: An Economical and Highly Active Catalyst for Ethanol Electrooxidation. *Sci. Rep.* **2013**, *3*, doi:10.1038/srep01181.
187. Assumpcao, M.; da Silva, S.G.; de Souza, R.F.B.; Buzzo, G.S.; Spinace, E.V.; Santos, M.C.; Neto, A.O.; Silva, J.C.M. Investigation of PdIr/C electrocatalysts as anode on the performance of direct ammonia fuel cell. *J. Power Sources* **2014**, *268*, 129–136.
188. Nguyen, S.T.; Yang, Y.H.; Wang, X. Ethanol electro-oxidation activity of Nb-doped-TiO₂ supported PdAg catalysts in alkaline media. *Appl. Catal. B* **2012**, *113*, 261–270.
189. Liu, Y.Q.; Xu, C.X. Nanoporous PdTi Alloys as Non-Platinum Oxygen-Reduction Reaction Electrocatalysts with Enhanced Activity and Durability. *ChemSuschem* **2013**, *6*, 78–84.
190. Li, Y.S.; Zhao, T.S. A high-performance integrated electrode for anion-exchange membrane direct ethanol fuel cells. *Int. J. Hydrogen Energy* **2011**, *36*, 7707–7713.
191. Shen, S.Y.; Zhao, T.S.; Xu, J.B.; Li, Y.S. High performance of a carbon supported ternary PdIrNi catalyst for ethanol electro-oxidation in anion-exchange membrane direct ethanol fuel cells. *Energy Environ. Sci.* **2011**, *4*, 1428–1433.
192. Antolini, E.; Colmati, F.; Gonzalez, E.R. Ethanol oxidation on carbon supported (PtSn)(alloy)/SnO₂ and (PtSnPd)(alloy)/SnO₂ catalysts with a fixed Pt/SnO₂ atomic ratio: Effect of the alloy phase characteristics. *J. Power Sources* **2009**, *193*, 555–561.
193. Bambagioni, V.; Bianchini, C.; Marchionni, A.; Filippi, J.; Vizza, F.; Teddy, J.; Serp, P.; Zhiani, M. Pd and Pt-Ru anode electrocatalysts supported on multi-walled carbon nanotubes and their use in passive and active direct alcohol fuel cells with an anion-exchange membrane (alcohol = methanol, ethanol, glycerol). *J. Power Sources* **2009**, *190*, 241–251.

194. Zhang, Z.Y.; More, K.L.; Sun, K.; Wu, Z.L.; Li, W.Z. Preparation and Characterization of PdFe Nanoleaves as Electrocatalysts for Oxygen Reduction Reaction. *Chem. Mater.* **2011**, *23*, 1570–1577.
195. Tang, Y.F.; Zhang, H.M.; Zhong, H.X.; Ma, Y.W. A facile synthesis of Pd/C cathode electrocatalyst for proton exchange membrane fuel cells. *Int. J. Hydrogen Energy* **2011**, *36*, 725–731.
196. Jeyabharathi, C.; Venkateshkumar, P.; Mathiyarasu, J.; Phani, K.L.N. Carbon-Supported Palladium-Polypyrrole Nanocomposite for Oxygen Reduction and Its Tolerance to Methanol. *J. Electrochem. Soc.* **2010**, *157*, B1740–B1745.
197. Kumar, S.M.S.; Herrero, J.S.; Irusta, S.; Scott, K. The effect of pretreatment of Vulcan XC-72R carbon on morphology and electrochemical oxygen reduction kinetics of supported Pd nano-particle in acidic electrolyte. *J. Electroanal. Chem.* **2010**, *647*, 211–221.
198. Yin, S.B.; Cai, M.; Wang, C.X.; Shen, P.K. Tungsten carbide promoted Pd–Fe as alcohol-tolerant electrocatalysts for oxygen reduction reactions. *Energy Environ. Sci.* **2011**, *4*, 558–563.
199. Rao, C.V.; Viswanathan, B. Carbon supported Pd–Co–Mo alloy as an alternative to Pt for oxygen reduction in direct ethanol fuel cells. *Electrochim. Acta* **2010**, *55*, 3002–3007.
200. Sarkar, A.; Murugan, A.V.; Manthiram, A. Low cost Pd-W nanoalloy electrocatalysts for oxygen reduction reaction in fuel cells. *J. Mater. Chem.* **2009**, *19*, 159–165.
201. Zhou, Z.M.; Shao, Z.G.; Qin, X.P.; Chen, X.G.; Wei, Z.D.; Yi, B.L. Durability study of Pt–Pd/C as PEMFC cathode catalyst. *Int. J. Hydrogen Energy* **2010**, *35*, 1719–1726.
202. Chang, S.H.; Su, W.N.; Yeh, M.H.; Pan, C.J.; Yu, K.L.; Liu, D.G.; Lee, J.F.; Hwang, B.J. Structural and Electronic Effects of Carbon-Supported Pt_xPd_{1-x} Nanoparticles on the Electrocatalytic Activity of the Oxygen-Reduction Reaction and on Methanol Tolerance. *Chem. Eur. J.* **2010**, *16*, 11064–11071.
203. Sarapuu, A.; Kasikov, A.; Wong, N.; Lucas, C.A.; Sedghi, G.; Nichols, R.J.; Tammeveski, K. Electroreduction of oxygen on gold-supported nanostructured palladium films in acid solutions. *Electrochim. Acta* **2010**, *55*, 6768–6774.
204. Kariuki, N.N.; Wang, X.P.; Mawdsley, J.R.; Ferrandon, M.S.; Niyogi, S.G.; Vaughey, J.T.; Myers, D.J. Colloidal Synthesis and Characterization of Carbon-Supported Pd–Cu Nanoparticle Oxygen Reduction Electrocatalysts. *Chem. Mater.* **2010**, *22*, 4144–4152.
205. Fouda-Onana, F.; Bah, S.; Savadogo, O. Palladium-copper alloys as catalysts for the oxygen reduction reaction in an acidic media I: Correlation between the ORR kinetic parameters and intrinsic physical properties of the alloys. *J. Electroanal. Chem.* **2009**, *636*, 1–9.
206. Wei, Y.C.; Liu, C.W.; Chang, Y.W.; Lai, C.M.; Lim, P.Y.; Tsai, L.D.; Wang, K.W. The structure-activity relationship of Pd–Co/C electrocatalysts for oxygen reduction reaction. *Int. J. Hydrogen Energy* **2010**, *35*, 1864–1871.
207. Ohashi, M.; Beard, K.D.; Ma, S.G.; Blom, D.A.; St-Pierre, J.; van Zee, J.W.; Monnier, J.R. Electrochemical and structural characterization of carbon-supported Pt–Pd bimetallic electrocatalysts prepared by electroless deposition. *Electrochim. Acta* **2010**, *55*, 7376–7384.
208. Peng, Z.M.; Yang, H. Synthesis and Oxygen Reduction Electrocatalytic Property of Pt-on-Pd Bimetallic Heteronanostructures. *J. Am. Chem. Soc.* **2009**, *131*, 7542–7543.

209. Yang, J.H.; Zhou, W.J.; Cheng, C.H.; Lee, J.Y.; Liu, Z.L. Pt-Decorated PdFe Nanoparticles as Methanol-Tolerant Oxygen Reduction Electrocatalyst. *ACS Appl. Mater. Interfaces* **2010**, *2*, 119–126.
210. Yang, J.; Cheng, C.H.; Zhou, W.; Lee, J.Y.; Liu, Z. Methanol-Tolerant Heterogeneous PdCo@PdPt/C Electrocatalyst for the Oxygen Reduction Reaction. *Fuel Cells* **2010**, *10*, 907–913.
211. Li, W.Z.; Haldar, P. Supportless PdFe nanorods as highly active electrocatalyst for proton exchange membrane fuel cell. *Electrochem. Commun.* **2009**, *11*, 1195–1198.
212. Zhou, W.P.; Yang, X.F.; Vukmirovic, M.B.; Koel, B.E.; Jiao, J.; Peng, G.W.; Mavrikakis, M.; Adzic, R.R. Improving Electrocatalysts for O₂ Reduction by Fine-Tuning the Pt-Support Interaction: Pt Monolayer on the Surfaces of a Pd₃Fe(111) Single-Crystal Alloy. *J. Am. Chem. Soc.* **2009**, *131*, 12755–12762.
213. Jin, S.A.; Kwon, K.; Pak, C.; Chang, H. The oxygen reduction electrocatalytic activity of intermetallic compound of palladium-tin supported on tin oxide-carbon composite. *Catal. Today* **2011**, *164*, 176–180.
214. Sun, W.; Hsu, A.; Chen, R.R. Palladium-coated manganese dioxide catalysts for oxygen reduction reaction in alkaline media. *J. Power Sources* **2011**, *196*, 4491–4498.
215. Arroyo-Ramirez, L.; Rodriguez, D.; Otano, W.; Cabrera, C.R. Palladium Nanoshell Catalysts Synthesis on Highly Ordered Pyrolytic Graphite for Oxygen Reduction Reaction. *Acs Appl. Mater. Interfaces* **2012**, *4*, 2018–2024.
216. Jukk, K.; Alexeyeva, N.; Johans, C.; Kontturi, K.; Tammeveski, K. Oxygen reduction on Pd nanoparticle/multi-walled carbon nanotube composites. *J. Electroanal. Chem.* **2012**, *666*, 67–75.
217. Kim, Y.S.; Shin, J.Y.; Chun, Y.S.; Lee, C.; Lee, S.G. Anion-Dependent Electrocatalytic Activity of Supported Palladium Catalysts onto Imidazolium Salt-Functionalized Carbon Nanotubes in Oxygen Reduction Reaction. *Bull. Korean Chem. Soc.* **2011**, *32*, 3209–3210.
218. Seo, M.H.; Choi, S.M.; Kim, H.J.; Kim, W.B. The graphene-supported Pd and Pt catalysts for highly active oxygen reduction reaction in an alkaline condition. *Electrochem. Commun.* **2011**, *13*, 182–185.
219. Kim, D.; Ahmed, M.S.; Jeon, S. Different length linkages of graphene modified with metal nanoparticles for oxygen reduction in acidic media. *J. Mater. Chem.* **2012**, *22*, 16353–16360.
220. Gotoh, K.; Kawabata, K.; Fujii, E.; Morishige, K.; Kinumoto, T.; Miyazaki, Y.; Ishida, H. The use of graphite oxide to produce mesoporous carbon supporting Pt, Ru, or Pd nanoparticles. *Carbon* **2009**, *47*, 2120–2124.
221. Du, S.F.; Lu, Y.X.; Steinberger-Wilckens, R. PtPd nanowire arrays supported on reduced graphene oxide as advanced electrocatalysts for methanol oxidation. *Carbon* **2014**, *79*, 346–353.
222. Huang, S.Y.; Ganesan, P.; Popov, B.N. Electrocatalytic Activity and Stability of Titania-Supported Platinum-Palladium Electrocatalysts for Polymer Electrolyte Membrane Fuel Cell. *ACS Catal.* **2012**, *2*, 825–831.
223. Bae, S.J.; Nahm, K.S.; Kim, P. Electroreduction of oxygen on Pd catalysts supported on Ti-modified carbon. *Curr. Appl. Phys.* **2012**, *12*, 1476–1480.
224. Ramanathan, M.; Ramani, V.; Prakash, J. Kinetics of the oxygen reduction reaction on Pd₃M (M = Cu, Ni, Fe) electrocatalysts synthesized at elevated annealing temperatures. *Electrochim. Acta* **2012**, *75*, 254–261.

225. Wen, M.; Zhou, B.; Fang, H.; Wu, Q.S.; Chen, S.P. Novel-Phase Structural High-Efficiency Anode Catalyst for Methanol Fuel Cells: α -(NiCu)₃Pd Nanoalloy. *J. Phys. Chem. C* **2014**, *118*, 26713–26720.
226. Lee, K.R.; Jung, Y.; Woo, S.I. Combinatorial Screening of Highly Active Pd Binary Catalysts for Electrochemical Oxygen Reduction. *ACS Comb. Sci.* **2012**, *14*, 10–16.
227. Meng, H.; Shen, P.K. The beneficial effect of the addition of tungsten carbides to Pt catalysts on the oxygen electroreduction. *Chem. Commun.* **2005**, doi:10.1039/B506900A.
228. Meng, H.; Shen, P.K. Tungsten carbide nanocrystal promoted Pt/C electrocatalysts for oxygen reduction. *J. Phys. Chem. B* **2005**, *109*, 22705–22709.
229. Nie, M.; Shen, P.K.; Wu, M.; Wei, Z.D.; Meng, H. A study of oxygen reduction on improved Pt–WC/C electrocatalysts. *J. Power Sources* **2006**, *162*, 173–176.
230. Cui, G.F.; Shen, P.K.; Meng, H.; Zhao, J.; Wu, G. Tungsten carbide as supports for Pt electrocatalysts with improved CO tolerance in methanol oxidation. *J. Power Sources* **2011**, *196*, 6125–6130.
231. He, G.Q.; Yan, Z.X.; Ma, X.M.; Meng, H.; Shen, P.K.; Wang, C.X. A universal method to synthesize nanoscale carbides as electrocatalyst supports towards oxygen reduction reaction. *Nanoscale* **2011**, *3*, 3578–3582.
232. Pan, Y.; Zhang, F.; Wu, K.; Lu, Z.Y.; Chen, Y.; Zhou, Y.M.; Tang, Y.W.; Lu, T.H. Carbon supported Palladium-Iron nanoparticles with uniform alloy structure as methanol-tolerant electrocatalyst for oxygen reduction reaction. *Int. J. Hydrogen Energy* **2012**, *37*, 2993–3000.
233. Han, B.H.; Xu, C.X. Nanoporous PdFe alloy as highly active and durable electrocatalyst for oxygen reduction reaction. *Int. J. Hydrogen Energy* **2014**, *39*, 18247–18255.
234. Gobal, F.; Arab, R. A preliminary study of the electro-catalytic reduction of oxygen on Cu–Pd alloys in alkaline solution. *J. Electroanal. Chem.* **2010**, *647*, 66–73.
235. Yang, R.Z.; Bian, W.Y.; Strasser, P.; Toney, M.F. Dealloyed PdCu₃ thin film electrocatalysts for oxygen reduction reaction. *J. Power Sources* **2013**, *222*, 169–176.
236. You, D.J.; Jin, S.A.; Lee, K.H.; Pak, C.; Choi, K.H.; Chang, H. Improvement of activity for oxygen reduction reaction by decoration of Ir on PdCu/C catalyst. *Catal. Today* **2012**, *185*, 138–142.
237. Xiong, L.; Huang, Y.X.; Liu, X.W.; Sheng, G.P.; Li, W.W.; Yu, H.Q. Three-dimensional bimetallic Pd-Cu nanodendrites with superior electrochemical performance for oxygen reduction reaction. *Electrochim. Acta* **2013**, *89*, 24–28.
238. Lee, C.L.; Chiou, H.P.; Chang, K.C.; Huang, C.H. Carbon nanotubes-supported colloidal Ag–Pd nanoparticles as electrocatalysts toward oxygen reduction reaction in alkaline electrolyte. *Int. J. Hydrogen Energy* **2011**, *36*, 2759–2764.
239. Godinez-Garcia, A.; Perez-Robles, J.F.; Martinez-Tejada, H.V.; Solorza-Feria, O. Characterization and electrocatalytic properties of sonochemical synthesized PdAg nanoparticles. *Mater. Chem. Phys.* **2012**, *134*, 1013–1019.
240. Xu, L.; Luo, Z.M.; Fan, Z.X.; Zhang, X.; Tan, C.L.; Li, H.; Zhang, H.; Xue, C. Triangular Ag–Pd alloy nanoprisms: Rational synthesis with high-efficiency for electrocatalytic oxygen reduction. *Nanoscale* **2014**, *6*, 11738–11743.

241. Xu, J.B.; Zhao, T.S.; Li, Y.S.; Yang, W.W. Synthesis and characterization of the Au-modified Pd cathode catalyst for alkaline direct ethanol fuel cells. *Int. J. Hydrogen Energy* **2010**, *35*, 9693–9700.
242. Kim, D.S.; Kim, J.H.; Jeong, I.K.; Choi, J.K.; Kim, Y.T. Phase change of bimetallic PdCo electrocatalysts caused by different heat-treatment temperatures: Effect on oxygen reduction reaction activity. *J. Catal.* **2012**, *290*, 65–78.
243. Son, D.N.; Takahashi, K. Selectivity of Palladium-Cobalt Surface Alloy toward Oxygen Reduction Reaction. *J. Phys. Chem. C* **2012**, *116*, 6200–6207.
244. Ren, Y.B.; Zhang, S.C.; Fang, H.; Wei, X.; Yang, P.H. Investigation of Co₃O₄ nanorods supported Pd anode catalyst for methanol oxidation in alkaline solution. *J. Energy Chem.* **2014**, *23*, 801–808.
245. Liu, H.; Li, W.; Manthiram, A. Factors influencing the electrocatalytic activity of Pd_{100-x}Co_x (0 ≤ x ≤ 50) nanoalloys for oxygen reduction reaction in fuel cells. *Appl. Catal. B-Environ.* **2009**, *90*, 184–194.
246. Oishi, K.; Savadogo, O. Electrochemical investigation of Pd-Co thin films binary alloy for the oxygen reduction reaction in acid medium. *J. Electroanal. Chem.* **2013**, *703*, 108–116.
247. Barakat, N.A.M.; Abdelkareem, M.A.; Shin, G.; Kim, H.Y. Pd-doped Co nanofibers immobilized on a chemically stable metallic bipolar plate as novel strategy for direct formic acid fuel cells. *Int. J. Hydrogen Energy* **2013**, *38*, 7438–7447.
248. Tominaka, S.; Hayashi, T.; Nakamura, Y.; Osaka, T. Mesoporous PdCo sponge-like nanostructure synthesized by electrodeposition and dealloying for oxygen reduction reaction. *J. Mater. Chem.* **2010**, *20*, 7175–7182.
249. Serov, A.; Nedoseykina, T.; Shvachko, O.; Kwak, C. Effect of precursor nature on the performance of palladium-cobalt electrocatalysts for direct methanol fuel cells. *J. Power Sources* **2010**, *195*, 175–180.
250. Alia, S.M.; Jensen, K.O.; Pivovar, B.S.; Yan, Y.S. Platinum-Coated Palladium Nanotubes as Oxygen Reduction Reaction Electrocatalysts. *ACS Catal.* **2012**, *2*, 858–863.
251. Slanac, D.A.; Li, L.; Mayoral, A.; Yacaman, M.J.; Manthiram, A.; Stevenson, K.J.; Johnston, K.P. Atomic resolution structural insights into PdPt nanoparticle-carbon interactions for the design of highly active and stable electrocatalysts. *Electrochim. Acta* **2012**, *64*, 35–45.
252. Chen, X.T.; Jiang, Y.Y.; Sun, J.Z.; Jin, C.H.; Zhang, Z.H. Highly active nanoporous Pt-based alloy as anode and cathode catalyst for direct methanol fuel cells. *J. Power Sources* **2014**, *267*, 212–218.
253. Lim, B.; Jiang, M.J.; Camargo, P.H.C.; Cho, E.C.; Tao, J.; Lu, X.M.; Zhu, Y.M.; Xia, Y.N. Pd–Pt Bimetallic Nanodendrites with High Activity for Oxygen Reduction. *Science* **2009**, *324*, 1302–1305.
254. Tang, Y.F.; Gao, F.M.; Yu, S.X.; Li, Z.P.; Zhao, Y.F. Surfactant-free synthesis of highly methanol-tolerant, polyhedral Pd–Pt nanocrystallines for oxygen reduction reaction. *J. Power Sources* **2013**, *239*, 374–381.
255. Limpattayanate, S.; Hunsom, M. Effect of supports on activity and stability of Pt–Pd catalysts for oxygen reduction reaction in proton exchange membrane fuel cells. *J. Solid State Electrochem.* **2013**, *17*, 1221–1231.

256. Thanasilp, S.; Hunsom, M. Effect of Pt: Pd atomic ratio in Pt–Pd/C electrocatalyst-coated membrane on the electrocatalytic activity of ORR in PEM fuel cells. *Renew. Energy* **2011**, *36*, 1795–1801.
257. Ficicilar, B.; Bayrakceken, A.; Eroglu, I. Effect of Pd loading in Pd–Pt bimetallic catalysts doped into hollow core mesoporous shell carbon on performance of proton exchange membrane fuel cells. *J. Power Sources* **2009**, *193*, 17–23.
258. Ang, S.Y.; Walsh, D.A. Palladium-vanadium alloy electrocatalysts for oxygen reduction: Effect of heat treatment on electrocatalytic activity and stability. *Appl. Catal. B* **2010**, *98*, 49–56.
259. Li, B.; Prakash, J. Oxygen reduction reaction on carbon supported Palladium-Nickel alloys in alkaline media. *Electrochem. Commun.* **2009**, *11*, 1162–1165.
260. Zhao, J.; Sarkar, A.; Manthiram, A. Synthesis and characterization of Pd–Ni nanoalloy electrocatalysts for oxygen reduction reaction in fuel cells. *Electrochim. Acta* **2010**, *55*, 1756–1765.
261. Miah, M.R.; Masud, J.; Ohsaka, T. Kinetics of oxygen reduction reaction at electrochemically fabricated tin-palladium bimetallic electrocatalyst in acidic media. *Electrochim. Acta* **2010**, *56*, 285–290.
262. Kim, J.; Park, J.E.; Momma, T.; Osaka, T. Synthesis of Pd–Sn nanoparticles by ultrasonic irradiation and their electrocatalytic activity for oxygen reduction. *Electrochim. Acta* **2009**, *54*, 3412–3418.
263. Karan, H.I.; Sasaki, K.; Kuttiyiel, K.; Farberow, C.A.; Mavrikakis, M.; Adzic, R.R. Catalytic Activity of Platinum Mono layer on Iridium and Rhenium Alloy Nanoparticles for the Oxygen Reduction Reaction. *ACS Catal.* **2012**, *2*, 817–824.
264. Xiao, L.; Zhuang, L.; Liu, Y.; Lu, J.T.; Abruna, H.D. Activating Pd by Morphology Tailoring for Oxygen Reduction. *J. Am. Chem. Soc.* **2009**, *131*, 602–608.
265. Kondo, S.; Nakamura, M.; Maki, N.; Hoshi, N. Active Sites for the Oxygen Reduction Reaction on the Low and High Index Planes of Palladium. *J. Phys. Chem. C* **2009**, *113*, 12625–12628.
266. Erikson, H.; Sarapuu, A.; Alexeyeva, N.; Tammeveski, K.; Solla-Gullon, J.; Feliu, J.M. Electrochemical reduction of oxygen on palladium nanocubes in acid and alkaline solutions. *Electrochim. Acta* **2012**, *59*, 329–335.
267. Lee, C.L.; Chiou, H.P. Methanol-tolerant Pd nanocubes for catalyzing oxygen reduction reaction in H₂SO₄ electrolyte. *Appl. Catal. B* **2012**, *117*, 204–211.
268. Wang, D.L.; Xin, H.L.; Wang, H.S.; Yu, Y.C.; Rus, E.; Muller, D.A.; DiSalvo, F.J.; Abruna, H.D. Facile Synthesis of Carbon-Supported Pd–Co Core-Shell Nanoparticles as Oxygen Reduction Electrocatalysts and Their Enhanced Activity and Stability with Monolayer Pt Decoration. *Chem. Mater.* **2012**, *24*, 2274–2281.
269. Jang, J.H.; Pak, C.; Kwon, Y.U. Ultrasound-assisted polyol synthesis and electrocatalytic characterization of Pd_xCo alloy and core-shell nanoparticles. *J. Power Sources* **2012**, *201*, 179–183.
270. Koenigsmann, C.; Sutter, E.; Adzic, R.R.; Wong, S.S. Size- and Composition-Dependent Enhancement of Electrocatalytic Oxygen Reduction Performance in Ultrathin Palladium-Gold (Pd_{1-x}Au_x) Nanowires. *J. Phys. Chem. C* **2012**, *116*, 15297–15306.

271. Wang, J.X.; Inada, H.; Wu, L.J.; Zhu, Y.M.; Choi, Y.M.; Liu, P.; Zhou, W.P.; Adzic, R.R. Oxygen Reduction on Well-Defined Core-Shell Nanocatalysts: Particle Size, Facet, and Pt Shell Thickness Effects. *J. Am. Chem. Soc.* **2009**, *131*, 17298–17302.
272. Sasaki, K.; Naohara, H.; Cai, Y.; Choi, Y.M.; Liu, P.; Vukmirovic, M.B.; Wang, J.X.; Adzic, R.R. Core-Protected Platinum Monolayer Shell High-Stability Electrocatalysts for Fuel-Cell Cathodes. *Angew. Chem.-Int. Ed.* **2010**, *49*, 8602–8607.
273. Di Noto, V.; Negro, E. Synthesis, characterization and electrochemical performance of tri-metal Pt-free carbon nitride electrocatalysts for the oxygen reduction reaction. *Electrochim. Acta* **2010**, *55*, 1407–1418.
274. Rego, R.; Oliveira, M.C.; Alcaide, F.; Alvarez, G. Development of a carbon paper-supported Pd catalyst for PEMFC application. *Int. J. Hydrogen Energy* **2012**, *37*, 7192–7199.

© 2015 by the authors; licensee MDPI, Basel, Switzerland. This article is an open access article distributed under the terms and conditions of the Creative Commons Attribution license (<http://creativecommons.org/licenses/by/4.0/>).